Acta Pharmaceutica Sinica B 2024;14(1):273−291

Chinese Pharmaceutical Association
Institute of Materia Medica, Chinese Academy of Medical Sciences

Acta Pharmaceutica Sinica B

www.elsevier.com/locate/apsb
www.sciencedirect.com

ORIGINAL ARTICLE

Adiponectin restores the obesity-induced impaired immunomodulatory function of mesenchymal stromal cells *via* glycolytic reprogramming

Duc-Vinh Pham[a,b,†], Thi-Kem Nguyen[b,†], Bao-Loc Nguyen[b], Jong-Oh Kim[b], Jee-Heon Jeong[e], Inho Choi[c,d], Pil-Hoon Park[b,d,*]

[a]*Department of Pharmacology, Hanoi University of Pharmacy, Hanoi 100000, Viet Nam*
[b]*College of Pharmacy, Yeungnam University, Gyeongsan 38541, Republic of Korea*
[c]*Department of Medical Biotechnology, Yeungnam University, Gyeongsan 38541, Republic of Korea*
[d]*Research Institute of Cell Culture, Yeungnam University, Gyeongsan 38541, Republic of Korea*
[e]*Department of Precision Medicine, School of Medicine, Sungkyunkwan University, Suwon 16419, Republic of Korea*

Received 20 May 2023; received in revised form 7 August 2023; accepted 18 October 2023

KEY WORDS

Adiponectin;
Adipose-derived stromal cells;
Colitis;
Glycolytic induction;
HIF1α;
Immunomodulation;
Mesenchymal stromal cells;
Obesity

Abstract Obesity has been known to negatively modulate the life-span and immunosuppressive potential of mesenchymal stromal cells (MSC). However, it remains unclear what drives the compromised potency of obese MSC. In this study, we examined the involvement of adiponectin, an adipose tissue-derived hormone, in obesity-induced impaired therapeutic function of MSC. Diet-induced obesity leads to a decrease in serum adiponectin, accompanied by impairment of survival and immunomodulatory effects of adipose-derived MSC (ADSC). Interestingly, priming with globular adiponectin (gAcrp) improved the immunomodulatory potential of obese ADSC. Similar effects were also observed in lean ADSC. In addition, gAcrp potentiated the therapeutic effectiveness of ADSC in a mouse model of DSS-induced colitis. Mechanistically, while obesity inhibited the glycolytic capacity of MSC, gAcrp treatment induced a metabolic shift toward glycolysis through activation of adiponectin receptor type 1/p38 MAPK/hypoxia inducible factor-1α axis. These findings suggest that activation of adiponectin

*Corresponding author.
E-mail address: parkp@yu.ac.kr (Pil-Hoon Park).
[†]These authors made equal contributions to this work.
Peer review under the responsibility of Chinese Pharmaceutical Association and Institute of Materia Medica, Chinese Academy of Medical Sciences.

https://doi.org/10.1016/j.apsb.2023.10.019

signaling is a promising strategy for enhancing the therapeutic efficacy of MSC against immune-mediated disorders.

1. Introduction

Mesenchymal stromal cells (also known as mesenchymal stem cells, MSC) are classified as multipotent stem cells ubiquitously present in adult tissues, including adipose tissue and bone marrow[1]. Due to their multilineage differentiation capacity, MSC have long received great attention in tissue engineering and regenerative medicine. In addition, there has recently been huge interest in the robust immunomodulatory properties of MSC, making them an emerging treatment option for inflammatory and autoimmune disorders[2]. However, it should be noted that immunosuppression is not an intrinsic characteristic of MSC. High plasticity allows MSC to display distinct phenotypes and function in a disease microenvironment-dependent manner[3]. For example, pro-inflammatory cytokines, such as TNFα, IFNγ, and IL1β, have been reported to activate the immunosuppressive phenotype and enhance the anti-inflammatory potency of MSC[4]. Therefore, optimization of MSC therapy will require an understating of the various factors in disease microenvironment that affect the functional attributes of MSC.

Obesity, a metabolic disorder characterized by adipocyte hyperplasia and hypertrophy, has a significant impact on the local and systemic environment through the excessive production of pro-inflammatory cytokines/adipokines and aberrant recruitment of immune cells to dysfunctional adipose tissue[5]. Notably, obese microenvironment has been shown to negatively modulate the lifespan and pleiotropic functions of MSC[6–8]. Recent evidence also suggests that MSC derived from obese individuals are ineffective in the treatment of inflammation-associated conditions[9,10]. Given the physiological role of MSC as regulators of inflammatory and immune responses, certain obesity-associated complications, such as low-grade chronic inflammation, may be ascribed to dysfunction of MSC. However, it remains unclear which components in obese environment are responsible for the compromised potency of MSC. Furthermore, although numerous strategies have been developed to enhance the therapeutic potential of MSC, little has been known about the restoration of immunomodulatory properties of obese MSC.

Adipokines, a group of hormones derived from adipose-tissue, play diverse roles in the modulation of metabolism, energy expenditure, inflammation, and cardiovascular function[11]. In obese individuals, production of adipokines by adipose tissue becomes dysregulated, leading to elevated levels of pro-inflammatory adipokines but decreased expression of anti-inflammatory adipokines[12]. Adiponectin, whose expression is markedly downregulated during obesity, has received considerable attention owing to its key role in the control of metabolic homeostasis[13]. Recently, increasing evidence has suggested that adiponectin signaling regulates the fate and function of MSC. Indeed, adiponectin was found to support the survival of bone marrow MSC (BM-MSC) under unfavorable culture conditions such as hypoxia and serum deprivation through suppression of apoptotic cell death[14]. Moreover, adiponectin increased the resistance of BM-MSC to flow shear stress, which may have potential benefits in the improvement of MSC viability upon cardiac transplantation[15]. Intriguingly, the effectiveness of MSC therapy in the treatment of heart failure was reported to be dependent on the serum levels of adiponectin[16]. Furthermore, adiponectin signaling has been thought to critically contribute to the balance of osteogenesis/adipogenesis in MSC[17,18].

Although accumulating evidence supports various benefits of adiponectin in the survival and functional potency of MSC, the role of adiponectin in the modulation of anti-inflammatory and immunosuppressive functions in MSC is under-investigated. Likewise, the possible linkage between impaired adiponectin signaling and dysfunction of MSC during obesity remains elusive. Therefore, the present study aimed to investigate the effect of adiponectin on the survival and immunomodulatory function of adipose-derived MSC (ADSC) and to further determine whether dysregulated adiponectin is responsible for the impaired properties of MSC during obesity. We observed that adiponectin improved the immunomodulatory functions of ADSC by upregulating cell adhesion molecules, enhancing the production of soluble immunomodulators, and increasing cell viability under an inflammatory microenvironment. Interestingly, adiponectin restored the compromised immunomodulatory potency of obese ADSC *in vitro* and in mice with DSS-induced colitis. We also demonstrated that adiponectin potentiated the survival and function of lean and obese ADSC through cellular metabolic reprogramming toward aerobic glycolysis, mediated *via* activation of the Adiponectin receptor type1 (AdipoR1)/p38 MAPK/HIF1α signaling pathway.

2. Materials and methods

2.1. Chemicals and reagents

All reagents for cell culture were provided by Hyclone Laboratories (South Logan, UT, USA). Recombinant globular adiponectin (gAcrp; #450−21) was acquired from PeproTech (Rocky Hill, NJ, USA). PX-478 (#HY-10231) and NS-398 (#HY-13913) were purchased from MedChemExpress LLC (Monmouth Junction, NJ, USA). *N*ω-Nitro-L-arginine methyl ester (L-NAME; #N5751) was provided by Sigma−Aldrich (St. Louis, MO, USA). TNFα (#575202) and IFNγ (#575304) were procured from BioLegend (San Diego, CA, USA). Oligomycin (#11341) and 2-deoxy-D-glucose (#14325) were purchased from Cayman Chemical (Ann Arbor, MI, USA). SB203580 (#1202) and SP600125 (#1496) were obtained from Tocris Bioscience (Bristol, UK). U0126 (#9903) was procured from Cell Signaling Technology Inc (Beverly, MA, USA).

2.2. Animals

C57BL/6 mice (5- to 7-week-old) were purchased from Orient Ltd. (Osan, Republic of Korea). All animal experiments were

performed in adherence to the guidelines of the Yeungnam University Institutional Animal Care and Use Committee (IACUC). The experimental protocols were reviewed and approved by the Yeungnam University IACUC (Protocol number: 2022−015).

2.3. Isolation, culture, and characterization of ADSC

For isolation of mouse ADSC, inguinal adipose tissues were collected from 5- to 7-week-old C57BL/6 mice, followed by digestion with 0.1% collagenase P (#11213873001; Roche, Mannheim, Germany) in HBSS for 1 h at 37 °C with gentle shaking. The stromal vascular fraction (SVF) was then separated by centrifugation and treated with 1 × RBC lysis buffer to eliminate red blood cells. Cells from SVF were cultured in complete alpha-MEM. After overnight incubation, non-adherent cells were removed, and adherent cells were cultured until 80% confluency. The phenotype of the isolated ADSC was confirmed based on the positive expression of surface markers, including CD105, CD90, CD29, Sca-1, and CD44, and negative expression of CD11b, CD45, and CD34 (Supporting Information Fig. S1A−S11H). Multipotency of the isolated ADSC was further demonstrated by adipocyte (Fig. S1I), osteoblast (Fig. S1J), and chondrocyte (Fig. S1K) differentiation capacity using a Mouse Mesenchymal Stem Cell Functional Identification Kit (#SC010; R&D systems, Minneapolis, MN, USA).

Human ADSC (#STC002) were obtained from Stemore (Seoul, Republic of Korea). Mouse and human ADSC were routinely cultured in alpha-MEM containing 10% fetal bovine serum and 1% penicillin/streptomycin. Cells at passages between 3 and 5 were used for experiments.

2.4. Splenocyte/T cell isolation, activation, pre-licensing, and coculture with ADSC

Splenocytes were isolated from the spleen of 5- to 7-week-old C57BL/6 mice. Briefly, fresh spleens were minced into small pieces before being mashed through a 40-μm cell strainer. Cells were then treated with 1 × RBC lysis reagent to obtain splenocytes. In some experiments, pan $CD3^+$ T cells were purified from total splenocytes using a mouse CD3 T Cell Isolation Kit (#480023; BioLegend) according to the manufacturer's instructions. Splenocytes were first incubated with the biotin antibody cocktail, followed by further incubation with magnetic streptavidin nanobeads (15 min each on ice). The beads were separated from the $CD3^+$ cell suspension using a magnet. To monitor the proliferation of splenocyte/T cells, cells were fluorescent-labeled by incubation with 5 μmol/L of CFSE (#65-0850-84; Thermo Scientific, Waltham, MA, USA) for 10 min at room temperature. Splenocytes and T cells were cultured in RPMI media containing 10% FBS, 1% penicillin/streptomycin, and 50 μmol/L of 2-mercaptoethanol and activated with 1 μg/mL of phytohemagglutinin-L (#00-4977-93; ThermoScientific) or Dynabeads Mouse T-Activator CD3/CD28 (#11456D; Thermo Scientific) in the presence of 10 ng/mL of recombinant IL-2 (#575402; BioLegend).

For co-culture with splenocytes/T cells, ADSC were seeded in 24-well plates at different densities. After overnight incubation, cells were treated with gAcrp (0.1−1 μg/mL) for different periods in the serum-reduced media (containing 0.5% FBS). Cells were then washed three times with PBS to remove gAcrp trace before splenocytes/T cells (10^6 cells) were seeded into culture wells containing ADSC to obtain ADSC/splenocyte (or ADSC/T cells) ratios ranging from 1:5 to 1:80 depending on the experiments. The co-culture system was maintained in complete RPMI 1640 media containing lymphocyte activators, as described above.

2.5. Flow cytometry analysis

For staining the surface markers, cells were incubated with fluorescent-conjugated antibodies for 15 min on ice, followed by three washes with flow cytometry buffer (PBS containing 1% BSA). For detection of intracellular antigens, cells were fixed and permeabilized using the transcription-factor staining buffer (#00-5523-00; Thermo Scientific) before further incubation with fluorescent-conjugated antibodies for 30 min at room temperature. The antibodies used for flow cytometry analysis were APC anti-mouse CD3 (#100236), PE anti-mouse CD4 (#100408), FITC anti-mouse CD4 (#100405), Percyp-Cy5.5 anti-mouse CD8a (#155013), Percyp-Cy5.5 anti-mouse MHC-II (#116415), APC-cy7 anti-mouse/human CD11b (#101225), APC anti-mouse CD11c (117309), PE anti-mouse F4/80 (157303), APC anti-mouse PD-L1 (#124311), PE anti-mouse ICAM-1 (#116107), and APC anti-Foxp3 antibody (#MA5-16224). All these antibodies were purchased from BioLegend, except for the APC anti-Foxp3 antibody procured from Thermo Scientific (Waltham, MA, USA).

The proliferation rates of splenocytes/T cells were determined by CFSE dilution assay. After co-culture with ADSC, CFSE-labeled splenocytes/T cells were collected, stained with APC anti-CD3 antibody, and subjected to flow cytometry analysis. Live single $CD3^+$ cells were included in the final analysis. All flow cytometry experiments were performed with BD FACSCalibur or BD FACS Verse (BD Biosciences, San Jose, CA, USA) and proliferation index was calculated using Flowjo 7.6 software.

2.6. Cell viability assay

Cells were seeded in a 96-well plate at a density of 5000 cells/well. After overnight incubation, cells were treated as indicated in alpha-MEM containing 0.5% FBS. Finally, 20 μL of MTS reagent (#G3580; Promega Corporation, Madison, WI, USA) was directly added to the culture media. Cells were then incubated for further 2 h and absorbance was acquired at 490 nm using a microplate reader (BMG Labtech Inc., Ortenberg, Germany).

2.7. Measurement of ADP/ATP ratio

The ADP/ATP ratio was determined using ADP/ATP Ratio Assay Kit obtained from Sigma−Aldrich (#MAK135). Upon the indicated treatments, culture media were first replaced with ATP reagent and luminescence was read after 1 min (RLU_A) and 10 min (RLU_B) of incubation. ADP reagent was then added to culture wells, followed by measuring the luminescence after 1 min of incubation (RLU_C). The ADP/ATP was calculated as $(RLU_C - RLU_B)/RLU_A$.

2.8. Caspase-3 activity measurement

Caspase-3 activity was determined using a caspase-3/7 assay system (#G8091; Promega Corporation) according to the manufacturer's instructions. At the end of the treatment period, the luminogenic substrate Ac-DEVD-pNA was added to the cells in a 96-well white plate. The resultant luminescence produced from the cleavage of Ac-DEVD-pNA by caspase-3 was measured using a Spark™ 10 M multimode microplate reader (Tecan, Mannedorf, Switzerland).

2.9. Annexin V binding assay

Apoptotic cell death was determined using the Annexin V binding assay as previously described[19]. After treatments as indicated, cells were collected by trypsinization, followed by incubation with a staining solution containing FITC Annexin V (1 μg/mL) and 7-AAD (2.5 μg/mL) in binding buffer for 15 min at room temperature. The cells were then subjected to FACS analysis. Apoptotic cell populations were identified as FITC-positive or FITC/7-AAD-double positive.

2.10. Cell cycle analysis

Cells were seeded in a 60-mm dish at a density of 1.5×10^5 cells/dish. The treatments were performed in culture media containing 10% FBS. Cells were collected by trypsinization and fixed with 70% ice-cold ethanol for 2 h on ice. Subsequently, the cells were incubated with propidium iodide solution (50 μg/mL) containing RNAse I (550 U/mL) (#ab139418; Abcam, Cambridge, MA, USA) for 20 min at room temperature before being analyzed using flow cytometry in combination with Flowjo 7.6 software.

2.11. Immunocytochemistry (ICC)

Subcellular localization of HIF1α was examined by ICC, as described previously[20]. Cells were fixed with 4% paraformaldehyde and permeabilized with 0.2% Triton-X100, followed by sequential incubation with a primary antibody against HIF1α (#NB100-479; Novus Biologicals, Centennial, CO, USA) and Alexa fluor 488 conjugated secondary antibody (#ab150077; Abcam). The nuclei were counterstained with DAPI. Images were acquired using a confocal microscope (Confocal microscope A1, Nikon, Tokyo, Japan).

2.12. Western blot analysis

Total cellular extracts were prepared using RIPA buffer (#89900; Thermo Scientific) containing a protease inhibitor cocktail, and protein concentrations were quantified using a BCA protein assay kit (#23227; Thermo Scientific). Sodium dodecyl sulfate (SDS) polyacrylamide gel electrophoresis and immunoblotting analysis were carried out as previously described[21]. Briefly, equal amounts of proteins were resolved on SDS polyacrylamide gel by electrophoresis before being transferred to a PVDF membrane. The membranes were then sequentially incubated with a primary antibody (4 °C, overnight) and an HRP-conjugated secondary antibody (room temperature, 1 h). The resultant immunocomplexes were detected by an enhanced chemiluminescent (ECL) system (#34580; Thermo Scientific) using the Fujifilm LAS-4000 mini (Fujifilm, Tokyo, Japan).

Antibodies used for Western blot analysis were as follows: anti-AdipoR1 (#Sc518030), anti-AdipoR2 (#Sc514045), and anti-cyclin D1 (#Sc753) from Santa Cruz Biotechnology (Dallas, TX, USA); anti-HIF1α (#NB100-479) from Novus Biologicals; anti-β-actin (#MA5-15739) and anti-phospho-CK2 beta (#44-1090G) from Thermo Scientific; anti-CK2 beta from ABclonal Inc. (Woburn, MA, USA) (#A14722) anti-phospho-JNK (#9251), anti-JNK (#9258), anti-phospho-ERK (#4370), anti-ERK (#4695), anti-phospho-p38 MAPK (#9215), anti-p38 MAPK (#9212), anti-Bax (#5023), anti-Bcl2 (#3498), anti-cleaved caspase-3 (#9664), anti-mouse IgG (#7076), and anti-rabbit IgG (#7074) from Cell Signaling Technology Inc. (Beverly, MA, USA).

2.13. Transient knockdown with small interfering RNA (siRNA)

The cells were grown to a density of 50%−60% confluency. Transfection complexes of a target-gene specific siRNA or a scramble control siRNA were prepared using Lipofectamine RNAiMAX Transfection Reagent (#13778150; Thermo Scientific) according to the manufacturer's recommendations. Gene silencing efficiency was monitored by Western blot or flow cytometry analysis after 24−48 of transfection. All siRNA duplexes were designed and synthesized by Bioneer (Daejeon, Republic of Korea), and their sequences presented in Supporting Information Table S1.

2.14. Quantitative reverse transcription PCR (qRT-PCR)

Total RNA was extracted using Qiazol lysis reagent (#79306; Qiagen, Hilden, Germany). Complementary DNA (cDNA) was synthesized from total RNA (1 μg) using GoScript Reverse Transcriptase (#A5000; Promega Corporation). Relative gene expression was analyzed by quantitative PCR using the ABsolute qPCR SYBR Green Capillary Mix (#AB1285B; Thermo Scientific) in combination with a Roche LightCycler 2.0 (Mannheim, Germany). 18 S rRNA was used as a loading control. The primers used for PCR were synthesized by Bioneer. The sequences are shown in Table S1.

2.15. Measurement of nitrite/nitrate production and prostaglandin E2 (PGE2) release

Nitrite/nitrate, stable metabolites of nitric oxide (NO), and PGE2 were measured in culture media of ADSC monoculture or ADSC/splenocyte coculture. Nitrite/nitrate levels were determined using a Griess reagent system (#G2930; Promega Corporation). Briefly, culture media (50 μL) were mixed and incubated with an equal volume of sulfanilamide solution for 10 min, followed by addition of 50 μL of *N*-1-naphthylethylenediamine dihydrochloride (NED) solution to the reaction mixture. The formation of azo products was monitored by measuring the absorbance at 550 nm. PGE2 levels were determined using a PGE2 ELISA kit (#ADI-901-001; Enzo Biochem, Inc., Farmingdale, NY, USA) according to the manufacturer's guidelines. The nitrite/nitrate and PGE2 levels were calculated based on the standard curve prepared under the same conditions.

2.16. Measurement of oxygen consumption rate (OCR) and extracellular acidification rate (ECAR)

OCR and ECAR were monitored using the Extracellular Oxygen Consumption Assay Kit (#ab197243; Abcam) and Glycolysis Assay kit (#ab197244; Abcam), respectively. The cells were seeded in a 96-well black plate at a density of 3×10^4 cells/well. For OCR measurement, 10 μL of Extracellular O_2 Consumption Reagent was added to the fresh cell culture media, followed by sealing with 100 μL of high-sensitivity mineral oil. Fluorescence intensity was recorded at 380/650 nm every 90 s for 1 h. For determination of ECAR, 10 μL of Glycolysis Assay Reagent was added to the cells in the respiration buffer. ECAR was monitored by measuring the fluorescence intensity at 380/615 nm every 90 s for 1 h. The OCR and ECAR values were calculated as the slopes of fluorescence intensity *versus* time.

2.17. Generation of high-fat-diet (HFD) induced obese mice

To induce obesity, C57BL/6 mice were fed a high-fat diet (HFD) (60% fat, D12492), while lean mice were fed a standard diet.

Body weight was monitored weekly. Serum adiponectin and leptin levels were measured at different time points throughout the study. HFD feeding was maintained until significant changes in body weight and serum leptin/adiponectin levels were observed. At the end of the study, mice were sacrificed, and inguinal adipose tissues were collected for isolation of ADSC.

2.18. Determination of serum leptin and adiponectin levels

Serum adiponectin and leptin levels were measured in lean and obese mice using commercial ELISA kits for mouse adiponectin/Acrp30 (#DY1119) and mouse leptin (#DY498-05, R&D Systems (Minneapolis, MN, USA)). Briefly, blood samples were collected from tail veins. The serum was separated by centrifugation, appropriately diluted, and added into a high-binding 96-well plate precoated with a capture antibody. After incubation for 2 h, the sample solution was replaced with a solution containing detection antibody. The immunocomplexes were then conjugated with streptavidin-HRP and detected using TMB substrate (#421101; BioLegend). The concentrations of adiponectin and leptin were calculated from standard curves prepared using mouse recombinant adiponectin and leptin, respectively.

2.19. Development of DSS-induced colitis mouse model

Colitis was induced in 7-week-old C57BL/6 mice by administration of 3% DSS in drinking water for 7 days. Colitis mice were divided into five groups containing six mice in each group and received one of the following treatments: (1) ADSC from lean mice (lean ADSC); (2) ADSC from obese mice (obese ADSC); (3) lean ADSC modified by incubation with gAcrp for 6 h; (4) obese ADSC modified by incubation with gAcrp for 6 h; (5) PBS (disease control). In all treatments, ADSC were administered twice (on Days 1 and 3 after colitis induction) *via* peritoneal injection (3×10^6 cells per injection). Lean and obese ADSC were isolated from normal mice and HFD obese mice, as described above.

The mice were monitored daily for body weight changes and pathological signs, including diarrhea and rectal bleeding. Disease activity index (DAI) was calculated based on body weight loss, stool consistency, and bleeding severity as previously described[22]. On Day 9, mice were sacrificed, and colon tissue, spleen, and mesenteric lymph nodes were collected. Subsequently, single cells prepared from spleen and mesenteric lymph nodes were used for characterization of T regulatory cell (Treg) population by flow cytometry analysis. A part of the colon tissue was digested with collagenase P solution (0.1%, *w/v*) containing 0.1 mg/mL of DNAse I (#11284932001; Roche), and the resultant single cells were subjected to analyses of T cells, dendritic cells, and macrophages using flow cytometry. Other parts of the colon tissues were used for gene expression analyses by RT-qPCR, measurement of myeloperoxidase (MPO) activity, and histopathological examination.

2.20. Histopathological examination

Distal colon tissues were collected from all animals and kept in 4% paraformaldehyde for 24 h at 4 °C, followed by immersion in a 30% sucrose solution. Colon sections (20-μm thick) were prepared using a freezing sliding microtome (Microm HM 450, Thermo Scientific). After mounting on a gelatin-coated slide, the sections were sequentially stained with hematoxylin and eosin (H&E staining) using an H&E stain kit (#H-3502) from Vector Laboratories Inc. (Burlingame, CA, USA). Images were finally acquired using a light microscope (BX41 TF, Olympus, Tokyo, Japan). The histological score was calculated based on a grading scale as previously described[23].

2.21. Myeloperoxidase (MPO) activity assay

Colonic infiltration of neutrophils was examined by MPO activity assay. Colon tissue (10 mg) was homogenized in phosphate buffer (50 mmol/L) containing 0.5% hexadecyltrimethylammonium bromide using mechanical and ultrasonic homogenizers. After removing cell debris by centrifugation, tissue homogenates (50 μL) were mixed with 200 μL of 0.5 mmol/L *o*-dianisidine solution (#D3252; Sigma−Aldrich) containing 0.0001% H_2O_2 in a 96-well plate. The absorbance at 450 nm was monitored every 1 min for 5 min. The MPO activity was determined as the change in absorbance *versus* time according to a previously described method[23].

2.22. Measurement of ADSC colonic engraftment

For *in vivo* cell tracking, fluorescent labeling of ADSC was performed by incubating cells with 5 μmol/L of DiR (1,1′-dioctadecyl-3,3,3′,3′-tetramethylindotricarbocyanin iodide) for 15 min at 37 °C as previously described[24]. On Day 3 of colitis induction, DiR-labeled ADSC (3×10^6 cells) were administered to DSS-pretreated mice *via* intraperitoneal injection. After 48 h of treatment, colon tissues were isolated from all mice and the images were immediately acquired using IVIS Lumina III In Vivo Imaging System (PerkinElmer Inc., Waltham, MA, USA). Furthermore, single cells from colon tissues prepared as described above were subjected to flow cytometry analysis to determine the proportion of DiR positive cells.

2.23. Statistical analysis

All experiments were repeated at least three times. Data are expressed as mean ± standard error (SE). Statistical analyses were carried out with GraphPad Prism 8.02 (San Diego, CA, USA). Significant differences were indicated using one-way analysis of variance (ANOVA) or *t*-test (where only two conditions were compared). *P* values below 0.05 were considered to be statistically significant.

3. Results

3.1. Adiponectin enhances immunosuppressive potency of adipose-derived mesenchymal stem cells (ADSC) and restores obesity-induced impaired immunomodulatory function of ADSC

ADSC are known to modulate immune responses through suppression of lymphocyte proliferation. To investigate the effect of adiponectin on immunosuppressive potency of ADSC, we co-cultured control ADSC or globular adiponectin (gAcrp)-modified ADSC with splenocytes stimulated with phytohemagglutinin-L (PHA-L), a potent mitogen for lymphocytes. As shown in Fig. 1A, proliferation of splenocytes was significantly suppressed by co-culture with ADSC at ADSC/splenocyte ratios of 40 or lower. Importantly, gAcrp-preconditioned ADSC were superior to the control ADSC in suppressing splenocyte proliferation. To optimize the gAcrp priming condition for enhancing the immunosuppressive effect of ADSC, ADSC were stimulated with different concentrations of gAcrp for

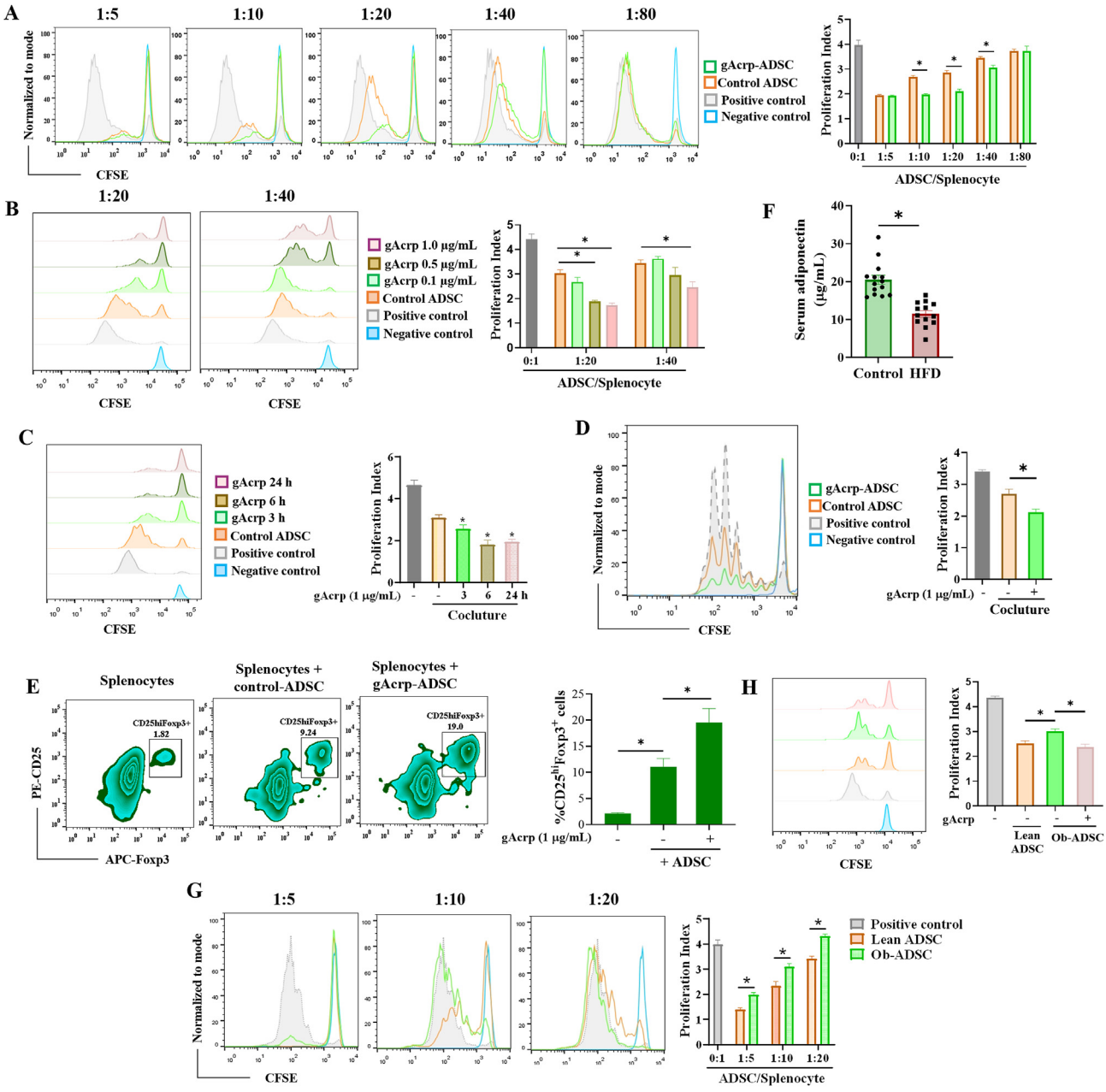

Figure 1 Effects of globular adiponectin on the immunomodulatory function of ADSC. (A) ADSC were seeded in a 24-well plate at different densities (0.125×10^5 to 2×10^5 cells/well) and pretreated with globular adiponectin (gAcrp) for 6 h, followed by coculturing with CFSE-labeled splenocytes (10^6 cells/well). Proliferation of lymphocytes was induced by supplementation of 1 μg/mL of PHA-l into coculture media. After 4 days of coculture, non-adherent cells were stained with an APC-conjugated anti-CD3 antibody and subjected to FACS analysis. Live and CD3-positive cell populations were selected for CFSE dilution analysis. (B) ADSC were preconditioned with different concentrations of gAcrp before coculturing with splenocytes at ADSC/splenocytes of 1:20 and 1:40. Proliferation of splenocytes was measured as described above. (C) ADSC were treated with 1 μg/mL of gAcrp for different time durations. At the end of treatment period, splenocytes were added into culture wells containing ADSC with a fixed ADSC/splenocytes ratio of 1:20. Lymphocyte proliferation was determined by CFSE dilution assay. (D) ADSC were incubated with 1 μg/mL of gAcrp for 6 h, followed by coculture with CFSE-stained mouse $CD3^+$ pan T cells (ADSC/splenocytes ratio of 1:20). T cells were activated with anti-CD3/CD28 beads in presence of IL-2 (10 ng/mL). The growth of T cells was examined after 4 days of coculture. (E) Mouse ADSC were stimulated with gAcrp (1 μg/mL, 6 h), followed by coculturing with non-labeled splenocytes for 4 days. Subsequently, splenocytes were subjected to immunofluorescent staining for anti-CD4 (FITC), CD25 (PE) and Foxp3 (APC). Dead cells were excluded by staining with a fixable viability dye. The proportion of CD25/Foxp3 double positive cell population among live and CD4-positive cells was determined. (F) C57BL/6 mice were fed with high-fat diet (HFD) for 12 weeks. After collection of blood samples from obese and lean mice, serum adiponectin was measured by ELISA. (G, H) ADSC derived from lean and obese mice were pretreated with gAcrp (1 μg/mL, for 6 h) and cocultured with CFSE-labeled splenocytes. PHA-stimulated lymphocyte proliferation was analyzed using CFSE dilution assay. $^*P < 0.05$ compared to indicated groups; $n = 3$ or $n = 13$ for Fig. 1F.

different durations prior to co-culture with splenocytes. The effect of gAcrp on immunomodulatory function of ADSC was found to be dose-dependent in a dose range between 0.1 and 1.0 μg/mL (Fig. 1B). Moreover, pretreatment of ADSC with gAcrp for 6 h was sufficient to produce an optimal stimulating effect on the immunosuppressive potential of ADSC (Fig. 1C). We next asked whether preconditioning was essential for the enhancement of ADSC immunosuppressive effects by adiponectin. Intriguingly, while adiponectin itself did not affect the proliferation of splenocytes, the supplementation of adiponectin into the ADSC-splenocyte co-culture system without pre-licensing also drastically inhibited PHA-induced lymphocyte growth (Supporting Information Fig. S2), implying that priming is not compulsory to enhance the immunomodulatory effects of ADSC by adiponectin. The role of adiponectin signaling in the immunomodulatory function of ADSC was further confirmed in an ADSC-T cell co-culture system, in which anti-CD3/anti-CD28 antibody-stimulated T cell proliferation was more potently suppressed by gAcrp-modified ADSC than in control ADSC (Fig. 1D). In addition, enhanced suppression of T cell proliferation by gAcrp pretreatment was observed in human ADSC (Supporting Information Fig. S3), suggesting that adiponectin signaling modulates the immunomodulatory function of both mouse and human ADSC.

ADSC have been postulated to modulate immune responses partly through the induction of regulatory T cells (Treg). Hence, we examined the effect of control and gAcrp-modified ADSC on the proportion of Treg population in ADSC-splenocyte co-culture. As expected, Treg population was significantly enriched in the ADSC-splenocyte coculture compared to that in splenocytes alone, which was further enhanced by pretreatment of ADSC with gAcrp (Fig. 1E). To further verify the Treg-inducing effect of gAcrp-modified ADSC, we co-cultured pan T cells with ADSC and determined the alterations in the gene expression of T cells. Consistent with Treg induction, T cells co-cultured with gAcrp-modified ADSC increased the expression of Treg markers, including Foxp3, IL-10, and TGFβ, but not other functional markers of T cells, such as TNFα and IFNγ (Supporting Information Fig. S4).

MSC derived from obese individuals exhibit morphological and functional abnormalities, which limits their therapeutic effectiveness. Given that adiponectin levels are decreased in obese individuals[25], dysregulated adiponectin signaling could be involved in dysfunction of MSC during obesity. To verify this hypothesis, we examined whether adiponectin restores the compromised function of MSC derived from the obese. For this purpose, we prepared high-fat diet (HFD)-induced obese mice. After 12 weeks of HFD feeding, obesity was confirmed by the overweight and elevated serum leptin levels (Supporting Information Fig. S5). Moreover, obese mice had significantly lower serum adiponectin levels than lean counterparts (Fig. 1F). Notably, obese ADSC exhibited a compromised immunosuppressive capacity, as evidenced by decreased suppressive effect on lymphocyte proliferation (Fig. 1G). Intriguingly, pre-licensing with gAcrp restored the dysregulated function of obese ADSC on suppressing lymphocyte proliferation (Fig. 1H). Collectively, these data demonstrated that adiponectin signaling leads to enhanced immunomodulatory effects of both lean and obese ADSC.

3.2. *Adiponectin enhances the therapeutic effectiveness of lean and obese ADSC in DSS-induced colitis mouse model*

The stimulatory effects of adiponectin on the anti-inflammatory and immunomodulatory potential of ADSC were validated *in vivo* in a DSS-induced colitis mouse model. In this model, colitis mice were treated with two intraperitoneal doses of lean ADSC, obese ADSC, gAcrp-primed lean ADSC, or gAcrp-primed obese ADSC (Fig. 2A). The severity of colitis was evaluated through body weight loss, colonic macroscopic and histological examination, as well as inflammation and immune response-related markers. As expected, administration of lean ADSC markedly ameliorated colitis symptoms, including body weight loss (Fig. 2B), disease activity index (Fig. 2C), colon shortening (Fig. 2D), and elevated MPO activity (Fig. 2E). Conversely, treatment with obese ADSC showed to be ineffective in the improvement of these pathological markers. Intriguingly, preconditioning with gAcrp substantially enhanced the therapeutic benefits of lean ADSC, but also restored the effectiveness of obese ADSC against DSS-induced colitis (Fig. 2B−E). Likewise, histological analysis also indicated that gAcrp-primed lean and obese ADSC more potently protected the damages in epithelial and crypt and suppressed colonic infiltration of immune cells compared to lean and obese control ADSC (Fig. 2F). Alterations in immune cell populations in the colon and lymphoid tissues were further characterized by flow cytometry analyses. While DSS-induced colitis led to downregulation of Treg cells in the mesenteric lymph nodes and spleen, lean ADSC, but not obese ADSC, drastically increased these cell populations (Fig. 2G). In addition, priming with gAcrp further enhanced Treg induction by lean ADSC, and restored the impaired effect of obese ADSC on positive modulation of Treg population. DSS-induced colitis is also characterized by high infiltration of $CD4^+$ and $CD8^+$ T cells, macrophages, and dendritic cells into the colon tissues. As expected, gAcrp pretreatment improved the suppressive effects of lean and obese ADSC on colonic infiltration of these immune cell populations (Fig. 2H and I). Consistent with FACS analyses, the superiority of gAcrp-primed ADSC over control ADSC in decreasing pro-inflammatory cytokines, such as TNFα, IFNγ, IL1β, IL6, and IL17, and increasing anti-inflammation- and Treg-induction related markers, including TGFβ, IL10, and Foxp3 (Fig. 2J and Supporting Information Fig. S6), were confirmed by RT-qPCR analysis. More importantly, priming with gAcrp restored all these defective functions in obese ADSC. Taken together, the present findings reveal that pre-silencing with gAcrp is effective to enhance therapeutic efficacy of lean and obese ADSC in the treatment of DSS-induced colitis.

3.3. *Adiponectin increases immunosuppressive potency of ADSC through promoting secretion of soluble factors and cell-to-cell contact*

It has been postulated that immunomodulatory activities of MSC are mediated *via* secretome and/or contact-dependent inhibition[26]. To elucidate the mechanism by which adiponectin enhances the immunosuppressive effect of MSC, we examined the proliferation of splenocytes in a Transwell-based co-culture system of splenocyte-ADSC. As shown in Fig. 3A, ADSC co-cultured with splenocytes through a Transwell insert significantly suppressed splenocyte proliferation, confirming the non-contact lymphocyte inhibition ability of ADSC. Notably, while adiponectin enhanced the lymphocyte suppressive activity of ADSC in the Transwell-based co-culture, this enhancement was drastically lower than that in the direct co-culture. These findings suggest that adiponectin increases immunoregulatory potency of ADSC through both cell-to-cell contact and stimulating the secretion of soluble factors. To further verify this notion, we examined the effect of adiponectin on the expression of immunomodulation-related genes and found that adiponectin upregulated the expression and

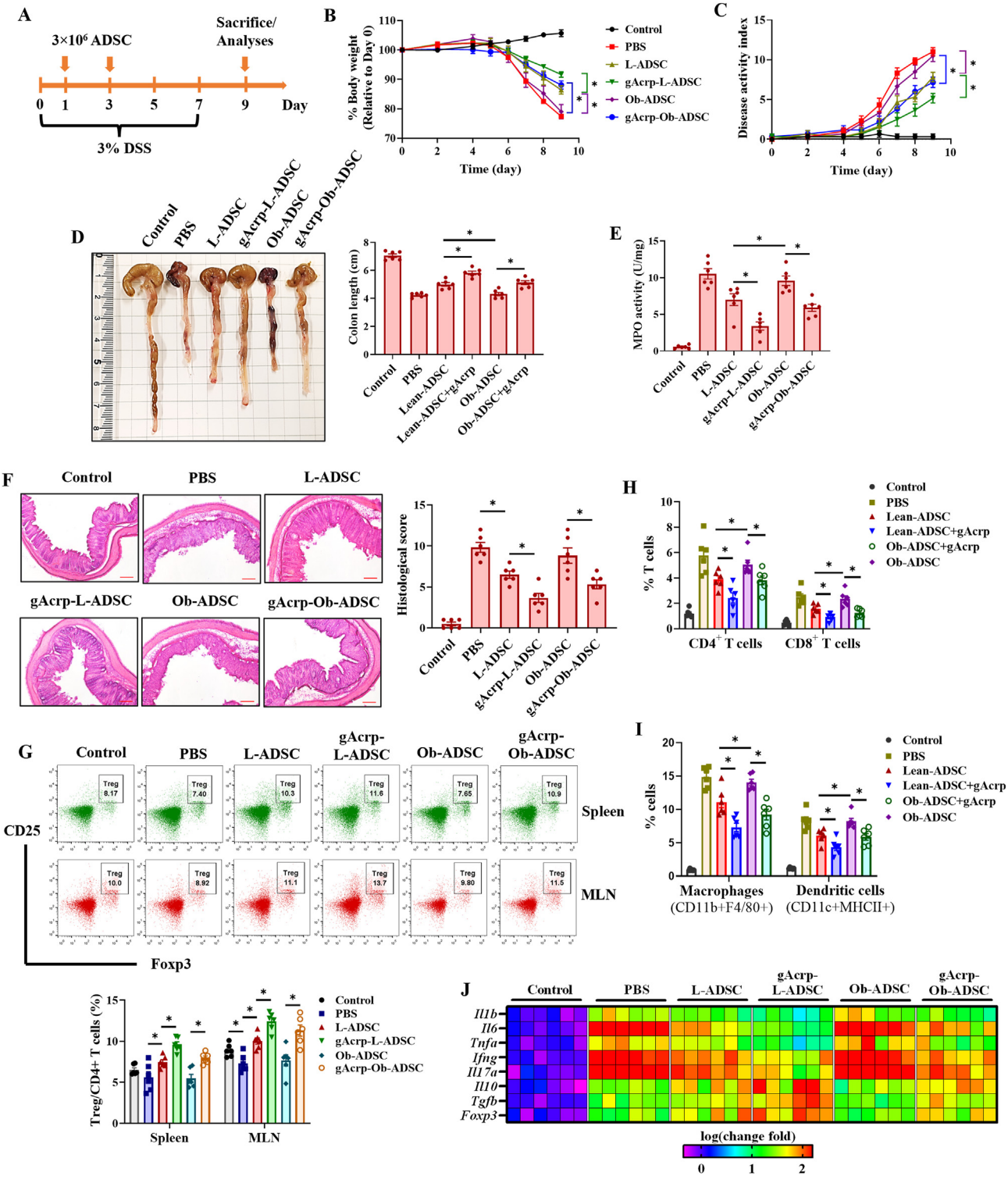

Figure 2 Therapeutic effectiveness of lean and obese ADSC modified with globular adiponectin against DSS-induced colitis. (A) Experiment scheme for the *in vivo* study. Colitis was induced in C57BL/6 mice by administration of 3% DSS in drinking water for 7 days. Colitis mice received one of the following treatments: PBS (DSS control), lean ADSC (L-DSC), gAcrp-modified lean ADSC (gAcrp-L-ADSC), obese ADSC (Ob-ADSC), and gAcrp-modified obese ADSC (gAcrp-Ob-ADSC). All treatments were administered two times on Days 1 and 3 (3×10^6 cells each dose) *via* intraperitoneal injection. On Day 9, mice were sacrificed, and colon tissues were collected for further investigations. (B) Body weight was monitored throughout the study and changes in body weight compared to Day 0 were presented. (C) Disease activity index was calculated based on the status of stool, bleeding, and body weight loss, as indicated in Methods. (D) Representative images of colon from each group were presented (left panel). Colon lengths in each group were indicated in the bar graph (right panel). (E) MPO activity in colon tissues was determined. (F) Colon tissues were subjected to H&E staining. Representative images for each group were presented (left panel) along with

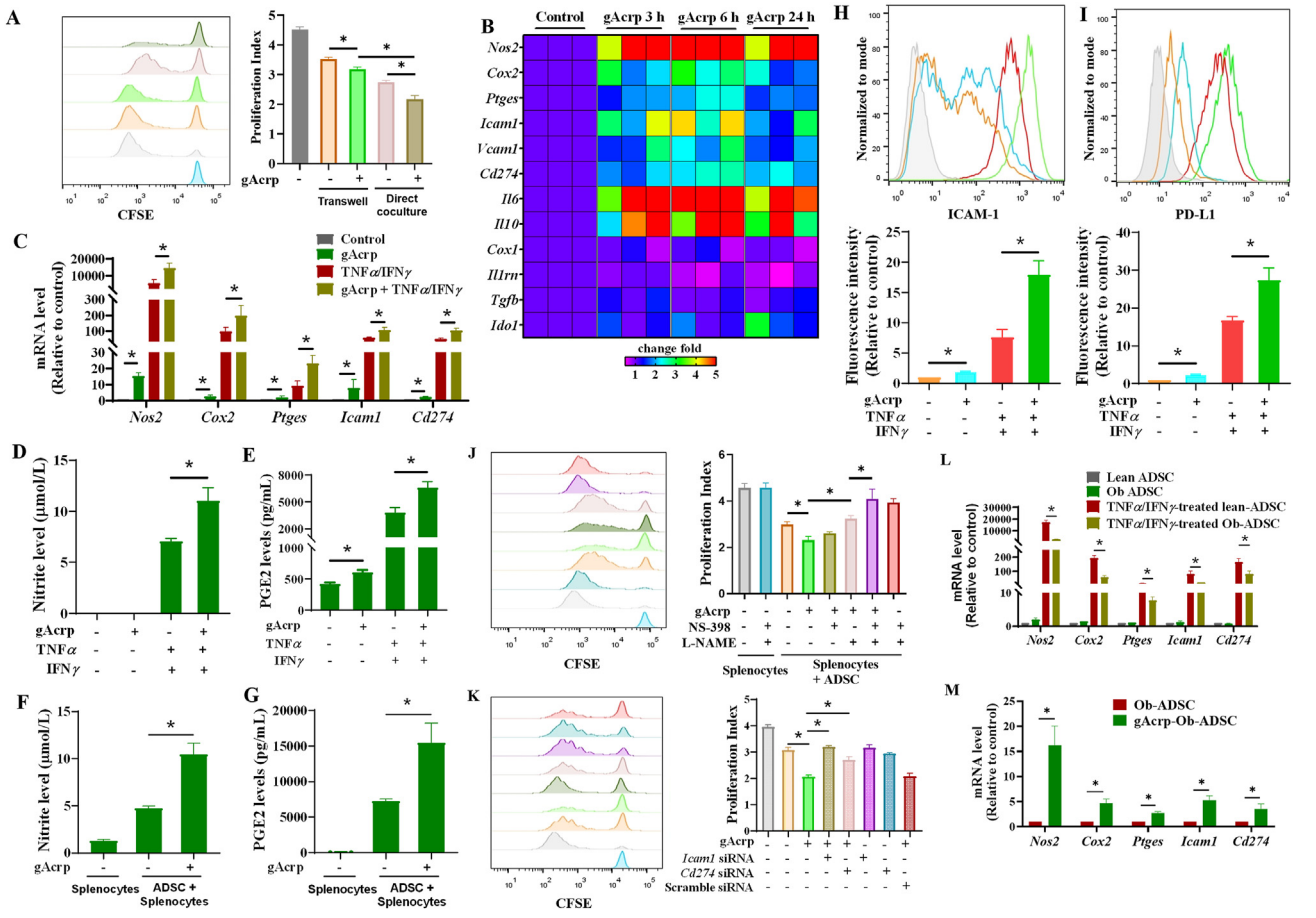

Figure 3 Involvement of both soluble factors and cell-to-cell contact in modulating immunosuppressive potency of ADSC by globular adiponectin. (A) ADSC were pretreated with gAcrp for 6 h, followed by coculturing with splenocytes (ADSC/splenocytes of 1:20) directly or through a transwell insert to prevent cell-to-cell contact. PHA-stimulated lymphocyte proliferation was examined by CFSE dilution assay as described above. (B) ADSC were treated with 1 μg/mL of gAcrp for indicated periods. The messenger RNA levels of immunomodulation-related genes were measured by RT-qPCR and demonstrated in a figure representing the fold changes. Quantification data for each gene are presented in Fig. S7. (C−E) ADSC were pretreated with gAcrp for 6 h, followed by further stimulation with TNFα (10 ng/mL) and IFNγ (20 ng/mL) for 24 h (C) or 48 h (D, E). (C) Expression levels of *Nos2*, *Cox2*, *Ptges*, *Icam1*, *and Cd274* were determined using RT-qPCR. (D, E) Nitrite/nitrate (D) and prostaglandin E2 (PGE2) (E) levels in culture media were measured as described in the Methods. (F, G) ADSC were preconditioned with gAcrp for 6 h, followed by coculturing with PHA-activated splenocytes. The concentrations of nitrate/nitrite (F) and PGE2 (G) in coculture media were examined after 3 days of coculture. (H, I) ADSC were pretreated with gAcrp for 6 h and further stimulated with TNFα/IFNγ for 24 h. Membrane ICAM-1 (H) and PD-L1 (I) were determined by labelling with respective fluorophore-conjugated antibodies, followed by flow cytometry analysis. (J) ADSC were treated with gAcrp for 6 h, followed by coculturing with PHA-activated splenocytes. NS-398 (10 μmol/L), a COX-2 inhibitor, and L-NAME, an inhibitor of iNOS, were supplemented to coculture media. Lymphocyte proliferation rate was measured at Day 4 of coculture. (K) ADSC were transfected with siRNA targeting *Icam1* or *Cd274*. After 24 h, cells were treated with gAcrp for further 6 h and cocultured with PHA-activated splenocytes for 4 days. Lymphocyte proliferation rate was finally monitored as described in Methods. (L) The mRNA levels of *Nos2*, *Cox2*, *Ptges*, *Icam1*, and *Cd274* were determined in ADSC derived from lean and obese mice with or without TNFα/IFNγ stimulation. (M) Obese ADSC were treated with gAcrp (1 μg/mL) for 6 h and the expression of indicated genes was measured by RT-qPCR. The knockdown efficiency of ICAM-1 and PD-L1 was examined by flow cytometry analysis (Fig. S9). $*P < 0.05$ compared to indicated groups; $n = 3$.

histological injury scores determined as described in Methods (right panel). (G) Single cells were isolated from spleens and mesenteric lymph nodes (MLN) of all mice at the end of the study. Cells were then stained with anti-CD4 (FITC), anti-CD25 (PE), and anti-Foxp3 (APC) antibody. Representative images for $CD25^{+}Foxp3^{hi}$ population among $CD4^{+}$ cells from each group were shown (left panel) along with the proportion of Treg (right panel). (H, I) Colon tissues were digested with collagenase to obtain single cells. Cells were stained either with anti-CD3 (APC), anti-CD4 (PE), and anti-CD8 (Percp-Cy5.5) antibody cocktail (H), or with anti-MHC-II (Percp-Cy5.5), anti-CD11b (APC-Cy7), anti-CD11c (APC), and anti-F4/80 (PE) antibody cocktail (I). The percentage of $CD4^{+}$ T cells ($CD3^{+}CD4^{+}$ population), $CD8^{+}$ T cells ($CD3^{+}CD8^{+}$ population), macrophages ($CD11b^{+}F4/80^{+}$ population), and dendritic cells ($MHC\text{-}II^{+}CD11c^{+}$ population) among colon-derived single cells was determined using FACS analysis. (J) The messenger RNA levels of indicated genes were measured in colon tissues by RT-qPCR and demonstrated in a figure representing fold changes. The quantification data for each gene are presented in Fig. S6. $*P < 0.05$ compared to indicated groups; $n = 6$.

secretion of various immunoregulatory factors, including iNOS (*Nos2*), COX-2, mPGES-1 (*Ptges*), IL-6, and IL-10, as well as membrane molecules, such as ICAM-1, VCAM-1, and PD-L1 (*Cd274*) (Fig. 3B and Supporting Information Fig. S7).

Pro-inflammatory cytokines, including TNFα and IFNγ, have been reported to activate immunosuppressive phenotype of MSC by inducing immunomodulation-related gene expression. Herein, we observed that adiponectin prominently increased the expression of various immunomodulatory genes. Intriguingly, it also significantly further enhanced the TNFα/IFNγ-stimulated expression of iNOS, COX-2, mPGES-1, ICAM-1, and PD-L1 (Fig. 3C), suggesting that adiponectin induces immunomodulation-related genes under basal and inflammatory conditions. Similar results were observed in ADSC derived from obese mice. In this study, stimulatory effects of obese-ADSC on immunomodulation-related genes in response to TNFα/IFNγ were lower than those of lean ADSC (Supporting Information Fig. S8A) but was recovered by pre-licensing with gAcrp (Fig. S8B). Consistent with the gene expression profile, adiponectin increased the levels of nitrite/nitrate, stable metabolites of nitric oxide (NO), and prostaglandin E2 (PGE2), an immunomodulator generated by COX-2 and mPGES1, either in the ADSC monoculture media (Fig. 3D and E) or in the co-culture media of ADSC and activated splenocytes (Fig. 3F and G). The inducing effects of adiponectin on membrane-located immuno-modulators, including ICAM-1 and PD-L1, were also confirmed by flow cytometry analyses (Fig. 3H and I). Finally, inhibitors of iNOS and COX-2, L-NAME and NS-398, abolished the suppressive effect of adiponectin-modified ADSC on lymphocyte proliferation (Fig. 3J). Moreover, gene silencing of ICAM-1 and PD-L1 also led to significant inhibition in the immunosuppressive effect of gAcrp-modified ADSC (Fig. 3K). Finally, we found that the induction of iNOS, COX2, mPGES-1, ICAM-1, and PD-L1 in response to TNFα/IFNγ stimulation was significantly impaired in obese ADSC compared to lean counterpart (Fig. 3L). Importantly, gAcrp retained its inducing effects on the expression of these genes in obese ADSC (Fig. 3M). Taken together, these findings imply that adiponectin potentiates the immunosuppressive activity of ADSC through increased production of NO and PGE2 or enhanced cell-to-cell contact through induction of membrane expression of ICAM-1 and PD-L1.

3.4. *Adiponectin enhances ADSC survival under inflammatory microenvironment*

Previous studies have shown that adiponectin enhances the viability of MSC under stressful conditions such as serum deprivation/hypoxia and flow shear stress[14,15]. Herein, we sought to investigate the modulatory effect of adiponectin on ADSC survival in an inflammatory microenvironment. We first confirmed that gAcrp enhanced the viability of serum-deprived ADSC in a time-dependent manner based on the MTS metabolic activity assay (Fig. 4A). In addition, treatment with gAcrp protected ADSC from serum-depletion-induced apoptosis (Fig. 4B), while it did not significantly affect cell cycle progression (Supporting Information Fig. S10), implying that adiponectin improves the viability of ADSC through suppression of apoptosis. The suppression of ADSC apoptosis by adiponectin was further verified by Western blot and caspase-3 activity assays, in which gAcrp caused marked downregulation of pro-apoptotic genes, including BAX and cleaved caspase-3, but upregulation of the anti-apoptotic gene BCL2 (Fig. 4C), and decreased caspase-3 activity in ADSC (Fig. 4D). Moreover, the pro-survival effect of gAcrp was observed in obese-derived ADSC. In this study, while obesity induced a significant increase in the apoptotic levels of ADSC under *in vitro* culture, gAcrp potently suppressed apoptosis of obese-ADSC, in which the apoptotic death in these cells returned to the levels similar to those of lean-ADSC (Fig. 4E).

To examine whether adiponectin promotes ADSC survival under inflammatory stimulation, we next measured apoptotic cell death in the presence of TNFα/IFNγ. TNFα/IFNγ supported the survival of ADSC in a low-serum medium by suppressing apoptosis (Supporting Information Fig. S11A). As corroborated by a decrease in the proportion of Annexin V-positive cells, gAcrp further suppressed the expression and activity of caspase-3 (Fig. S11B and S11C, respectively), as well as the regulation of apoptosis-related proteins, BAX and BCL2 (Fig. S11B). Likewise, gAcrp significantly decreased apoptotic ADSC population after three days of coculture with activated splenocytes (Fig. 4F). The enhancement of cell viability by gAcrp under inflammatory milieu was finally verified in DSS-induced colitis mice using fluorescent labeling technique in combination with *in vivo* imaging. Peritoneal injection of ADSC induced the subsequent colonic migration and engraftment. Interestingly, priming with gAcrp led to an increase in the number of colon engrafted ADSC (Fig. 4G). The flow cytometry analysis was then confirmed that the proportion of live ADSC in colon tissues after 48 h of transplantation was significantly higher in gAcrp-primed lean and obese ADSC compared to untreated lean and obese control cells, respectively (Fig. 4H). Taken together, these findings suggest that adiponectin improves immunoregulatory function of ADSC, at least in part, through enhanced cell viability in an inflammatory microenvironment.

3.5. *HIF1α mediates the improved survival and function of ADSC by adiponectin*

Compelling evidence delineates that HIF1α plays a critical role in the survival and immunomodulatory function of MSC[27]. Adiponectin induces HIF1α expression in macrophages[21]. To elucidate the mechanisms underlying enhanced viability and function of MSC by adiponectin, we speculated on the role of HIF1α signaling. To this end, we first demonstrated the induction of HIF1α by gAcrp in ADSC in the absence (Fig. 5A) and presence (Fig. 5B) of inflammatory stimuli. The HIF1α inducing effect of adiponectin was further confirmed by confocal imaging showing that adiponectin increased nuclear levels of HIF1α in ADSC under both basal and TNFα/IFNγ-activated conditions (Fig. 5C). Interestingly, HIF1α was found to be downregulated in obese ADSC compared to their lean counterparts (Fig. 5D), whereas treatment with gAcrp significantly restored HIF1α levels in these cells (Fig. 5E). Next, we verified the functional roles of HIF1α in modulation of immunosuppressive potency and survival of ADSC by adiponectin. As expected, blockage of HIF1α signaling using a specific siRNA or pharmacological inhibitor (PX-478) abrogated the beneficial effect of gAcrp on immunosuppressive activity of ADSC (Fig. 5F and G). Moreover, induction of immunomodulation-related genes, including *Nos2, Cox2, Ptges*, *Icam1*, and *Cd*274 by gAcrp was also significantly inhibited in HIF1α-deficient ADSC (Fig. 5H). Consistently, cobalt chloride ($CoCl_2$), a chemical inducer of HIF1α, also enhanced the suppressive effect of ADSC on splenocyte proliferation (Supporting Information Fig. S12A) and induced expression of immunomodulation-related genes (Fig. S12B). We finally conducted a series of experiments to confirm the crucial role of HIF1α in the enhanced ADSC survival by adiponectin. Gene

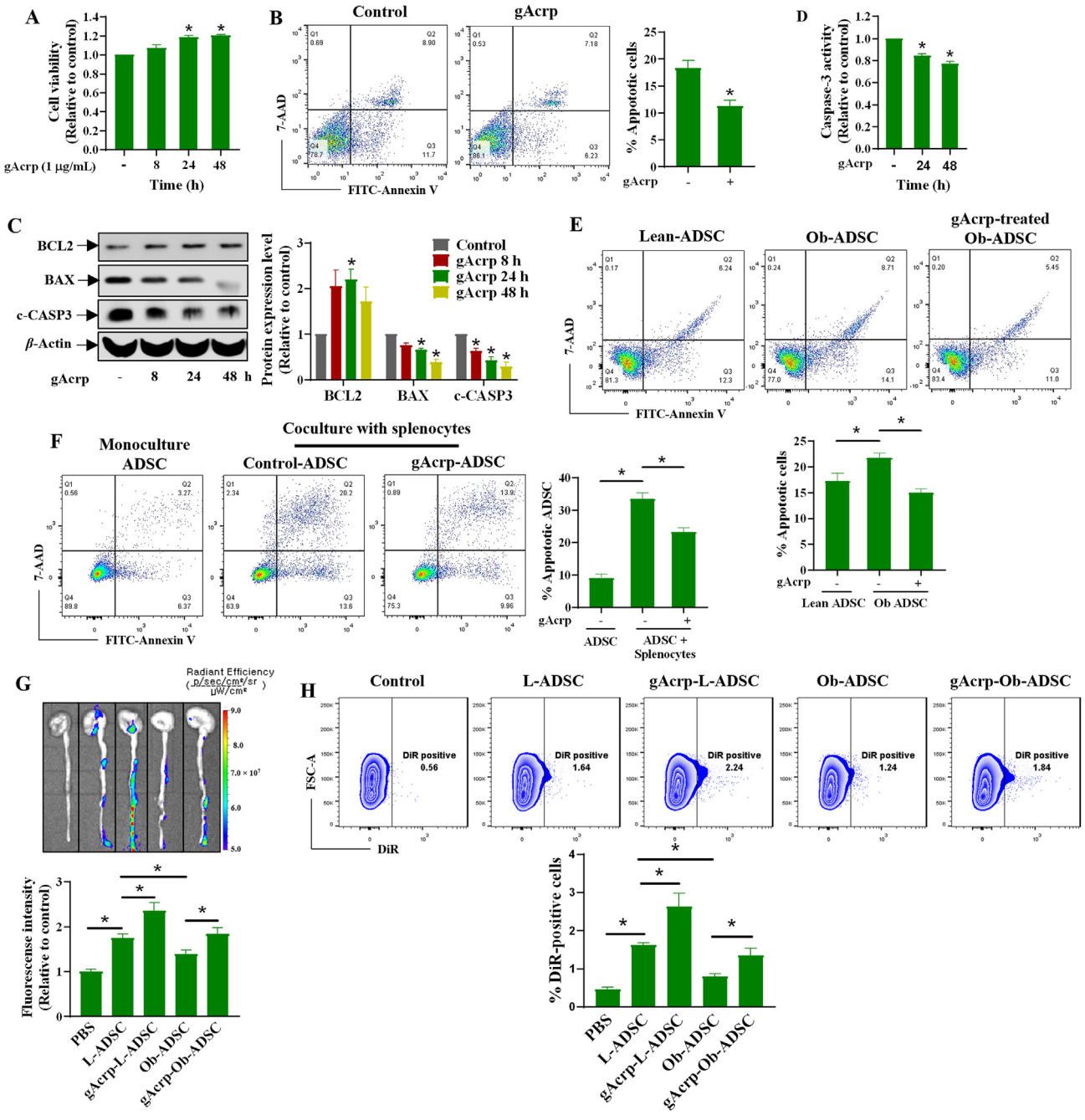

Figure 4 Pro-survival effects of globular adiponectin on ADSC under inflammatory microenvironment. (A) After treatment with gAcrp for different time periods, viability of ADSC was examined by MTS assay. (B) ADSC were treated with gAcrp for 48 h. The proportion of apoptotic cells was determined by Annexin V binding assay. (C, D) ADSC were treated with gAcrp for different time periods. (C) Expression levels of BCL2, BAX, and cleaved caspase-3 (c-CASP3) were measured by Western blot analysis. (D) The caspase-3 activity was measured as described in Methods. In experiments A−D, cell death was induced by culturing in low-serum (0.5% FBS) containing media. (E) ADSC derived from obese mice were treated with gAcrp for 48 h. Proportion of apoptotic cells was determined by Annexin V binding assay. (F) ADSC were treated with gAcrp for 6 h, followed by coculturing with anti-CD3/CD28-activated splenocytes. After 3 days of coculture, adherent cells were collected by trypsinization, and then sequentially labeled with anti-CD45 (APC) antibody and FITC-Annexin V/7-AAD. Proportion of apoptotic cell death in CD45-negative cells was determined by flow cytometry analysis. (G, H) Colitis was induced in C57BL/6 by supplementation of 3% DSS in drinking water. After 3 days of colitis induction, mice were intraperitoneally injected with 3×10^6 DiR-labeled ADSC from lean and obese mice with or without gAcrp preconditioning. PBS was used as negative control. On Day 5, colon tissues were collected for fluorescent imaging analysis, followed by preparation of single cells for flow cytometry analysis. (G) Representative images of colon tissues were shown along with the quantitation of relative DiR fluorescent intensity in colon tissues from all mice. (H) Single cells were subjected to FACS analysis for determining the proportion of DiR-positive live cells. $^*P < 0.05$ compared to indicated groups; $n = 3$ (A−F) or 4 (G, H).

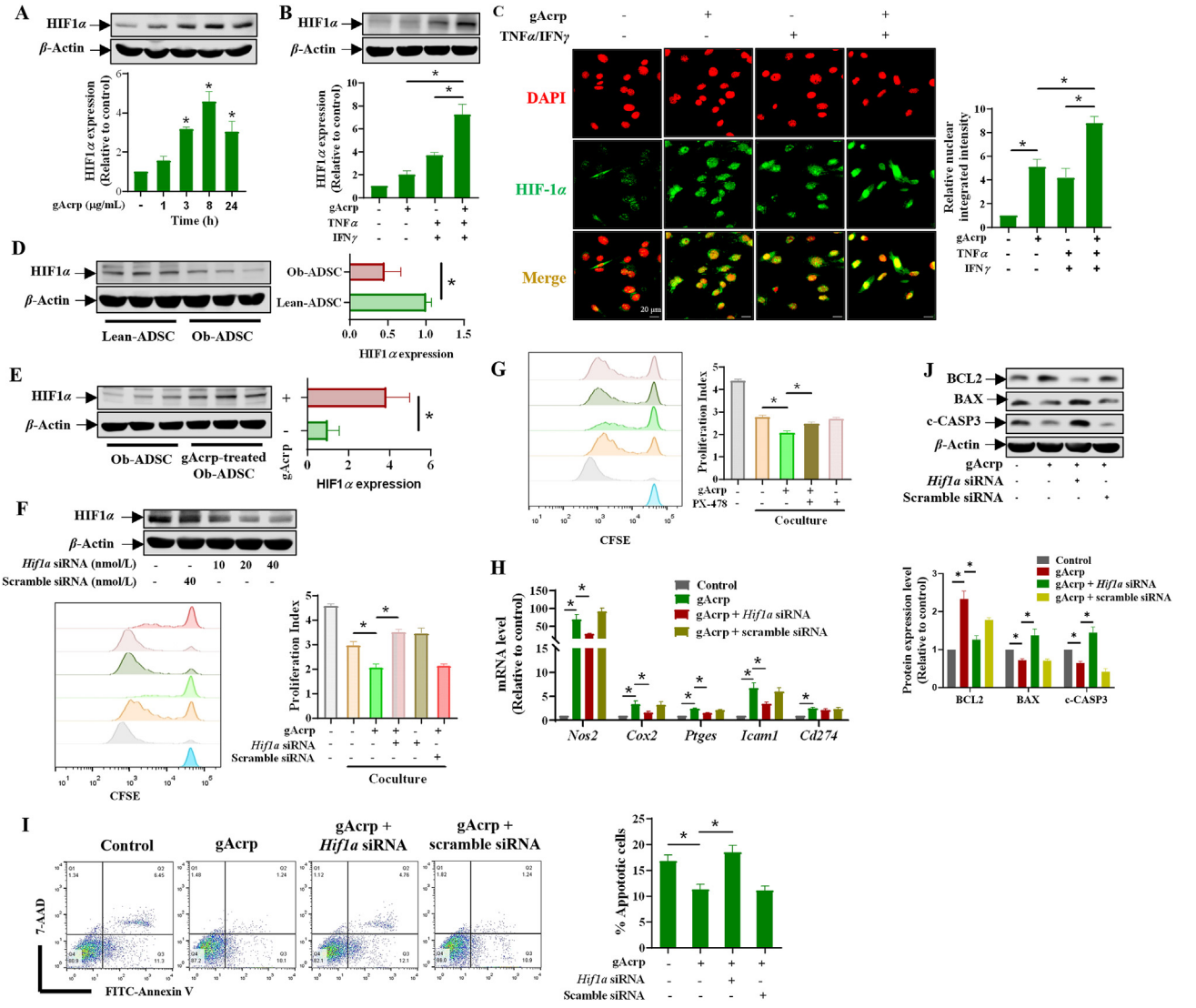

Figure 5 Critical roles of HIF1α signaling in the enhanced cell viability and immunosuppressive function of ADSC by globular adiponectin. (A, B) ADSC were treated with gAcrp for indicated time periods (A) or pretreated with gAcrp for 6 h and then stimulated with TNFα/IFNγ for additional 24 h (B). HIF1α expression was measured by Western blot analysis. (C) ADSC were treated with gAcrp alone or in combination with TNFα/IFNγ for 24 h. Cells were immunolabeled with an anti-HIF1α primary antibody and an Alexa fluor 488-conjugated secondary antibody (green), followed by counterstaining with DAPI (red). Subcellular distribution of HIF1α was analyzed using a confocal microscope. Representative images from three independent experiments were presented in upper panel. The nuclear integrated intensity of HIF1α was analyzed using Image J software and presented in the bar diagram (lower panel). Scale bar: 20 μm. (D, E) Expression levels of HIF1α in lean and obese ADSC in the absence (D) or presence (E) of gAcrp were determined by Western blot analysis. (F, G) (F) ADSC were transfected with siRNA targeting *Hif1a* (20 nmol/L) for 24 h, followed by treatment with gAcrp for additional 6 h. Gene silencing efficiency was monitored by Western blot analysis (upper panel). (G) Cells were pretreated with PX-478 (50 μmol/L) (G), a pharmacological inhibitor of HIF1α, for 2 h, followed by treatment with gAcrp for further 6 h. ADSC were then cocultured with CFSE-labeled splenocytes in presence of mitogen PHA-l. Lymphocyte proliferation was examined on Day 4 of coculture using FACS analysis. (H) ADSC were transfected with *Hif1a* siRNA (20 nmol/L) for 24 h, and then treated with gAcrp for 6 h. The expression levels of *Nos2*, *Cox2*, *Ptges*, *Icam1*, and *Cd274* were examined by RT-qPCR. (I, J) ADSC were transfected with *Hif1a* siRNA. After 24 h of incubation, cells were further stimulated with gAcrp for 48 h. (I) The percentage of apoptotic cells was determined using Annexin V binding assay. (J) Expression levels of apoptosis-related proteins were evaluated by Western blot analysis. $^*P < 0.05$ compared to indicated groups; $n = 3$.

silencing of HIF1α or pretreatment with HIF1α inhibitor (PX-478) abolished the enhancement of cell viability by gAcrp (Supporting Information Fig. S13). Similarly, the anti-apoptotic effects of adiponectin, as determined by annexin staining (Fig. 5I) and measurement of caspase-3 activity and expression levels of BCL-2, BAX, and cleaved caspase-3 (Fig. 5J), were also abrogated by knockdown of HIF1α. Together, these findings reveal that HIF1α induction is essentially required for the improvement of the immunosuppressive potency and pro-survival effects of adiponectin in ADSC.

3.6. HIF1α upregulation improves cell viability and function of ADSC through induction of glycolysis

HIF1α is a key regulator of cellular energy metabolism[28]. We assumed that adiponectin modulates the fate of ADSC through HIF1α-dependent cellular metabolic reprogramming. To this end, we examined the effect of gAcrp on the balance of glycolysis/oxidative phosphorylation (OXPHOS) by measuring extracellular acidification rate (ECAR) and oxygen consumption rate (OCR). Interestingly, gAcrp increased ECAR, but reduced OCR (Fig. 6A and B), indicating a metabolic shift from OXPHOS to glycolysis in the gAcrp-treated ADSC. In addition, co-treatment of ADSC with gAcrp and TNFα/IFNγ enhanced glycolytic induction by these cytokines (Fig. 6C), suggesting that adiponectin drives the cellular metabolic program of ADSC in an inflammatory microenvironment. These notions were further supported by the finding that gAcrp increased ADP/ATP ratio in ADSC in the absence or presence of TNFα/IFNγ co-stimulation (Supporting Information Fig. S14). HIF1α is thought to regulate glycolytic flux by promoting the transcription of glycolysis-related genes, such as *Slc2a1* (*Glut1*), *Pdk1*, and *Ldha*. In consistent, we observed that gAcrp increased the mRNA levels of these genes in the absence or presence of TNFα/IFNγ (Fig. 6D). The functional role of HIF1α in glycolysis induction by adiponectin was further confirmed in HIF1α knockdown cells. As shown in Fig. 6, gene silencing of HIF1α significantly abrogated the shifting effect of gAcrp from OCR to ECAR (Fig. 6E), as well as mRNA levels of *Slc2a1*, *Pdk1*, and *Ldha* (Fig. 6F). In line with previous findings showing the downregulation of HIF1α in obese-derived ADSC, these cells presented a metabolic shift toward OXPHOS as evidenced by reduced glycolysis but increased OCR. Importantly, gAcrp restored the metabolic profile of obese ADSC by enhancing their glycolytic capacity (Fig. 6G).

Next, we verified the contribution of glycolytic induction to the enhancement of survival and immunomodulatory function of ADSC by adiponectin. To this end, we compared the effects of oligomycin (Omy), an inhibitor of OXPHOS, and 2-deoxy-D-glucose (2-DG), an inhibitor of glycolysis, on apoptosis in control and gAcrp-treated ADSC. As shown in Fig. 6H, Omy appeared to suppress apoptosis of ADSC, as evidenced by a decrease in caspase-3 activity. Notably, caspase-3 activity was also decreased by Omy in gAcrp-treated ADSC, in which caspase-3 activity was lower than that in the control, indicating that the anti-apoptotic effect of gAcrp was maintained in the presence of Omy. In contrast, both control and gAcrp-treated ADSC were sensitive to 2-DG to enhance caspase-3 activity, in which no significant difference in caspase-3 activity was observed between control and gAcrp-treated ADSC (Fig. 6I), indicating that gAcrp failed to prevent apoptosis of ADSC in the presence of 2-DG. The Annexin V binding assay also confirmed that 2-DG, but not Omy, abolished the suppressive effect of gAcrp on apoptotic cell death in ADSC (Fig. 6J). Finally, we found that pretreatment with 2-DG prevented the additive effect of gAcrp on immunosuppressive potency of ADSC based on the splenocyte proliferation assay. In this study, as expected, Omy treatment showed no significant effect on suppression of lymphocyte proliferation by gAcrp-modified ADSC, while it increased the immunosuppressive effect in control ADSC (Fig. 6K). Collectively, these results clearly indicate that adiponectin induces the glycolytic phenotype in ADSC, which is essential for maintenance of survival and immunomodulatory function of ADSC.

3.7. Activation of AdipoR1/p38 MAPK axis contributes to HIF1α induction and enhanced immunosuppression in ADSC

Having demonstrated the critical role of HIF1α signaling in adiponectin-modulation of ADSC survival and immunomodulatory function, we next sought to unveil the mechanism underpinning HIF1α induction by adiponectin. While both adiponectin receptor 1 (AdipoR1) and adiponectin receptor 2 (AdipoR2) are expressed in ADSC, gene silencing of *Adipor1*, but not *Adipor2*, significantly suppressed immunosuppressive potency of gAcrp-modified ADSC, as corroborated by decreased lymphocyte suppressive capacity (Fig. 7A) and reduced expression of immunomodulation-related genes (Fig. 7B). These results suggest that activation of AdipoR1, rather than AdipoR2, is required for the beneficial effects of gAcrp on the cell viability and immunomodulatory function of ADSC. In attempts to identify the downstream signaling pathways of AdipoR1, we examined the involvement of MAPK, AMPK, and CK2 signaling pathways, which are well-known downstream effectors of AdipoR1/2, and found that adiponectin induced activation of ERK, JNK, and p38 MAPK (Fig. 7C), as well as AMPK and CK2β (Supporting Information Fig. S15A). Interestingly, only SB203580, a pharmacological inhibitor of p38 MAPK, markedly abrogated the stimulatory effect of gAcrp on lymphocyte suppressive activity of ADSC without significant effects by inhibitors of ERK, JNK (Fig. 7D), CK2, and AMPK (Fig. S15B and S15C). Moreover, upregulation of immune modulation-related genes by gAcrp was inhibited by pretreatment with SB203580 (Fig. 7E), indicating that activation of p38 MAPK contributes to the positive modulation of ADSC function by adiponectin. It is also worth noting that gAcrp failed to activate p38 MAPK in *Adipor1* deficient ADSC (Fig. 7F), suggesting that phosphorylation of p38 MAPK is controlled by adiponectin/AdipoR1 signaling. Regarding the role of AdipoR1/p38 MAPK axis in modulation of ADSC viability, we observed that the enhanced survival of gAcrp-treated ADSC was abrogated either by knockdown of AdipoR1 or by pretreatment with SB203580 (Supporting Information Fig. S16). Finally, we demonstrated that HIF1α induction by gAcrp was abolished by transfection with *Adipor1* siRNA (Fig. 7G) or a p38 MAPK inhibitor (Fig. 7H). Taken together, these results suggest that adiponectin increases cell viability and immunomodulatory function of ADSC *via* activation of the AdipoR1/p38 MAPK/HIF1α signaling pathway.

4. Discussion

Adiponectin, a hormone predominantly secreted by adipose tissue, modulates the fate of MSC by enhancing cell viability under stressful conditions and controlling the balance of adipogenic/osteogenic differentiation. However, little has been known about the role of adiponectin signaling in the determination of MSC immunomodulatory potency and the effectiveness of MSC therapy in the treatment of inflammatory/immune disorders. In this study, we demonstrated that adiponectin potentiated the immunosuppressive properties of ADSC through remodeling cellular metabolic programs toward glycolysis. Moreover, adiponectin restores dysregulated immunomodulatory functions and enhances apoptotic cell death of ADSC derived from obese mice. Given that adiponectin plasma levels are significantly decreased in obese individuals, the results of the present study provide the first evidence that impaired adiponectin signaling would be implicated in

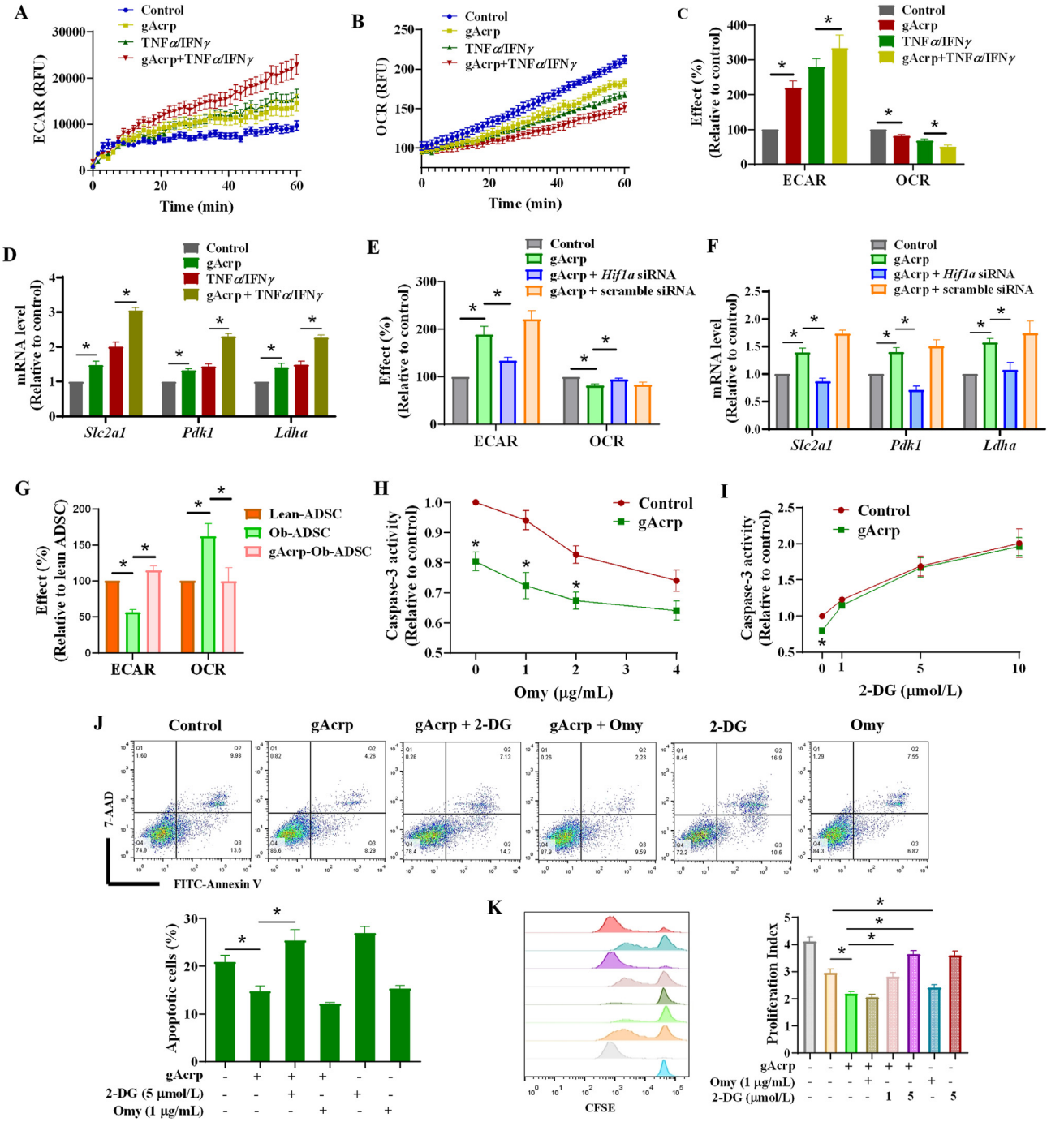

Figure 6 Involvement of HIF1α-driven glycolytic induction in the enhanced survival and function of ADSC by globular adiponectin. (A–D) ADSC were pretreated with gAcrp for 6 h, followed by stimulation with TNFα/IFNγ (10 and 20 ng/mL, respectively) for additional 24 h, or treated with gAcrp alone for 24 h. Extracellular acidification rate (ECAR) (A) and oxygen consumption rate (OCR) (B) were measured as described in Methods. (C) Relative ECAR and OCR compared to the control were shown. (D) Expression levels of *Slc2a1*, *Pdk1*, and *Ldha* were examined by RT-qPCR assay. (E, F) ADSC were transfected with *Hif1a* siRNA (20 nmol/L) for 24 h, followed by treatment with gAcrp for further 24 h. (E) ECAR and OCR were measured as described above and their values relative to control group were presented. (F) The messenger RNA levels of *Slc2a1*, *Pdk1*, and *Ldha* were determined by RT-qPCR. (G) ECAR and OCR were examined in obese ADSC treated with gAcrp in comparison with those in lean counterparts. (H–J) ADSC were pretreated with oligomycin (Omy) or 2-deoxy-D-Glucose (2-DG) at indicated concentrations for 2 h, followed by treatment with gAcrp (1 μg/mL) for additional 24 h. (H, I) The caspase-3 activity was determined as described above. (J) The apoptotic levels were measured using Annexin V binding assay. (K) ADSC were pretreated with Omy and 2-DG as indicated, followed by further incubation with 1 μg/mL of gAcrp for 6 h. ADSC were then cocultured with CFSE-labeled splenocytes in presence of PHA-l. Lymphocyte proliferation was analyzed by CFSE dilution assay. *$P < 0.05$ compared to indicated groups; $n = 3$.

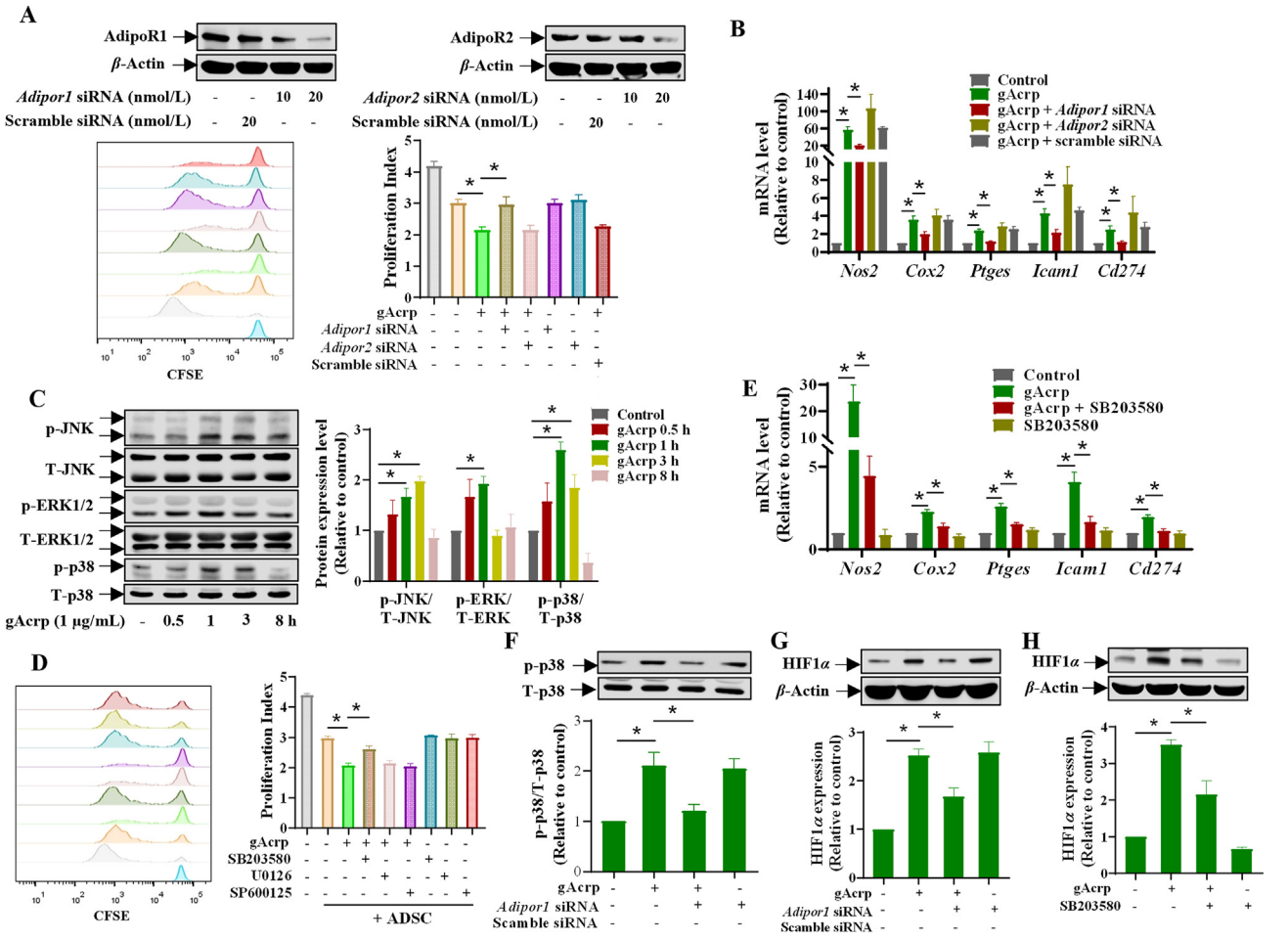

Figure 7 Induction of HIF1α and enhancement of ADSC potency by globular adiponectin are mediated *via* AdipoR1/p38 MAPK signaling pathways. (A) ADSC were transfected with siRNA targeting *Adipor1* or *Adipor2* (20 nmol/L) for 36 h, followed by treatment with gAcrp for further 6 h. Gene silencing efficiency was monitored by Western blot analysis (upper panel). *Adipor1*- or *Adipor2*-deficient ADSC were cocultured with CFSE-labeled splenocytes in presence of PHA-l. The proliferation rate of lymphocytes was measured by flow cytometry analysis (lower panel). (B) The mRNA expression levels of *Nos2*, *Cox2*, *Ptges*, *Icam1*, and *Cd274* were determined by RT-qPCR assay. (C) After treatment with gAcrp as indicated, total and phosphorylated levels of p38, ERK, and JNK were examined by Western blot analysis. (D) ADSC were pretreated with MAPK inhibitors, including U0126 (MEK inhibitor, 10 μmol/L), SB203580 (p38 MAPK inhibitor, 20 μmol/L), and SP600125 (JNK inhibitor, 20 μmol/L) for 2 h, followed by stimulation with gAcrp (1 μg/mL) for further 6 h. ADSC were then cocultured with PHA-activated splenocytes and lymphocyte proliferation was measured by CFSE dilution assay. (E) ADSC were pretreated with SB203580 for 2 h, followed by further treatment with gAcrp for 6 h. The mRNA levels of immunomodulation-related genes were determined by RT-qPCR. (F) ADSC were transfected with *Adipor1* siRNA for 36 h, followed by further incubation with gAcrp for 1 h (F). Total and phospho-p38MAPK levels were analyzed by Western blot analysis. (G, H) ADSC were transfected with *Adipor1* siRNA for 36 h (G) or pretreated with SB203580 for 2 h (H). The protein expression levels of HIF1α were determined by Western blot. $^*P < 0.05$ compared to indicated groups; $n = 3$.

the downregulation of immunomodulatory function of ADSC during obesity.

The therapeutic benefits of MSC were initially believed to be mainly attributable to their capacity to differentiate into cells in target tissue. However, their poor engraftment and low survival upon transplantation led to the re-evaluation of the mechanisms underlying beneficial effects of MSC in a context-specific manner[29]. Of the various pleiotropic functions, immunomodulatory properties make MSC a promising strategy for treating immune-mediated disorders[30]. On the other hand, since immunosuppressive potential of MSC can be enhanced by culture or environment engineering, great efforts have been made to improve the therapeutic efficacy of MSC[31]. Among them, modification of MSC with IFNγ with or without TNFα, which simulates activation of MSC by inflammatory microenvironment, is one of the best-established methods to potentiate the immunomodulatory function of MSC[32]. In the present study, we found that preconditioning with adiponectin could serve as a novel strategy to further improve the anti-inflammatory and immunosuppressive effects of ADSC. This notion was supported by the finding that adiponectin upregulated the genes coding for soluble and membrane-located immunoregulatory factors in both naïve and TNFα/IFNγ-activated ADSC (Fig. 3). Furthermore, activation of adiponectin signaling also supported the survival of ADSC under inflammatory environment by suppressing apoptosis (Fig. 4). Since previous studies have suggested that inflammatory milieu

accelerates the senescence of transplanted MSC[33,34], the pro-survival effect of adiponectin might critically contribute to the improvement of *in vivo* anti-inflammatory effectiveness of ADSC.

Given the role of adiponectin as a positive modulator of ADSC life-span and immunosuppressive potency, pathological conditions leading to decreased adiponectin levels are expected to affect the fate of resident ADSC and the effectiveness of MSC-based therapy. In this scenario, the most attention would focus on obesity, where production of adipokines, such as adiponectin, is dysregulated. Adiponectin was found to be downregulated in mice with HFD-induced obesity. In addition, ADSC derived from these mice showed compromised immunosuppressive potency and were ineffective in ameliorating DSS-induced colitis (Fig. 2). Importantly, modification of obese ADSC with adiponectin significantly restored their *in vitro* performance and *in vivo* anti-inflammatory potential. These findings imply that, although naïve ADSC from obese individuals might not be therapeutically effective, environmental engineering, such as preconditioning with adiponectin, allows the use of obese ADSC as an autologous cell source for the treatment of immune-mediated diseases. In fact, even though MSC are supposed to be immunoprivileged, immune rejection occurs during repetitive administration of allogeneic MSC[35,36]. Therefore, the development of methods for retraining obese MSC to retrieve their function would provide promising options for the optimization of MSC-based therapy in obese patients.

On the other hand, although DSS-induced colitis is one of the most widely used mouse models for investigating the immunoregulatory effect of MSC, the exact mechanism underlying their therapeutic benefits against colitis remains controversial. Therefore, while we demonstrated that precondition with gAcrp increased colonic engraftment of ADSC, suggesting that adiponectin confers the advantages of survival and/or homing ability to ADSC (Fig. 4G and H), the benefits by gAcrp priming are not essentially attributed to the enhanced cell viability. Indeed, it was initially believed that MSCs can be engrafted into injured tissues and thereby modify local inflammatory microenvironment through paracrine activity and direct contact with immune cells[37]. They were also supposed to have the capability to replace damaged cells of target organ. Conversely, Sala E. et al. demonstrated that MSCs did not significantly localize to the colon after intraperitoneal injection but formed the aggregates like spheroids in peritoneal cavity, which also contained immune cells such as macrophages and lymphocytes[38]. Interestingly, they revealed that production of certain cytokines from intraperitoneal aggregates of MSCs was responsible for therapeutic efficacy of MSCs in DSS-induced colitis, independent of the localization of MSCs in the intestine. A recent study also supports the notion that intraperitoneal administration of MSCs modulates colonic inflammation and immune responses indirectly through secreting factors[39]. Therefore, we supposed that not only increased cell viability but also improved immunomodulatory function contributed to higher therapeutic efficacy of gAcrp-primed ADSC.

Culture conditions for *in vitro* expansion of MSC have been shown to negatively impact their function. For example, MSC within stem cell niche are adapted to low oxygen concentrations (typically 1%−7%), whereas normoxic culture conditions optimize cell growth but also alter the morphological and functional properties of MSC[40]. Unsurprisingly, preconditioning with hypoxic conditions has been used to improve therapeutic potential of MSC, partly through upregulation of HIF1α[27,41]. To elucidate the molecular mechanism underlying the benefits of adiponectin priming in the improvement of ADSC therapeutic potential, we demonstrated that adiponectin promotes the expression of HIF1α under normoxic conditions *via* activation of the AdipoR1/p38 MAPK pathway. We further found that HIF1α induction by adiponectin essentially contributes to the enhancement of ADSC survival and function by inducing cellular metabolic reprogramming toward glycolysis. Intriguingly, previous reports showed that glycolytic phenotype supports immunosuppressive potency of MSC[42,43]. In addition, MSC appear to be largely dependent on glycolysis for energy production in nature but become more addictive to OXPHOS under *in vitro* expansion[44]. Therefore, our findings further confirm that maintenance of glycolytic flux by supplementation of adiponectin into culture media, other than known methods such as hypoxia induction and preconditioning with TNFα/IFNγ or oligomycin, can preserve metabolic and functional properties of MSC upon *in vitro* expansion.

Adiponectin acts *via* the transmembrane receptors AdipoR1, AdipoR2, and T-cadherin[45]. The affinity of adiponectin for these receptors is dependent on its existing form in circulation. In particular, only high-molecular-weight isoforms can bind to T-cadherin, while monomer isoforms and low-molecular-weight oligomers show equal binding ability to AdipoR1 and AdipoR2[45,46]. Conversely, globular adiponectin, a cleavage product of full-length adiponectin, possesses a higher affinity for AdipoR1 than the full-length forms, while its binding to AdipoR2 is still maintained[47]. Interestingly, most previous studies have reported that adiponectin modulates the viability and differentiation fate of MSC through AdipoR1[14,48], except for one study that propose activation of T-cadherin as a prerequisite for the enhanced therapeutic benefits of MSC by adiponectin in the treatment of cardiovascular disorder[16]. In line with previous reports, we also found that AdipoR1 activation is essential for adiponectin-modulation of ADSC survival and immunosuppressive function. Surprisingly, some effects of globular adiponectin in the present study (*e.g.*, pro-survival effect and iNOS induction) appears to be reinforced by gene silencing of AdipoR2 (Fig. 7B and Fig. S13). Although AdipoR1-and AdipoR2-specific actions are difficult to confirm due to deficiency in selective agonists for these receptors, our observations suggest that AdipoR2-mediated signaling pathways may also play roles in the modulation of MSC fate by adiponectin. In addition, we also asked whether AdipoRon, a synthetic AdipoR1/2 agonist, can be used as an alternative agent for recombinant adiponectin. In this study, we observed that AdipoRon improved the immunosuppressive properties of ADSC in a manner similar to gAcrp, as evidenced by induction of HIF1α (Supporting Information Fig. S17A), enhanced inhibition of splenocyte proliferation (Fig. S17B), and upregulation of immunoregulation-related genes (Fig. S17C). Given the critical roles of adiponectin receptor signaling in the determination of MSC function, adiponectin receptor agonists may serve as promising agents for enhancing the therapeutic potential of MSC.

Current evidence consistently demonstrates impairment in the survival and immunomodulatory functions of obese MSC. However, the detailed mechanisms by which obese environment induces the dysfunction of MSC are not completely understood. In the present study, we observed that ADSC from obese mice exhibited a metabolic shift from glycolysis to OXPHOS, possibly due to the downregulation of HIF1α signaling. These alterations were restored by incubation with adiponectin (Fig. 6), suggesting that decreased adiponectin levels and subsequent impaired adiponectin signaling during obesity are responsible, at least in part, for the detrimental effects of obese environment on MSC survival and function. Nevertheless, further studies are needed to verify

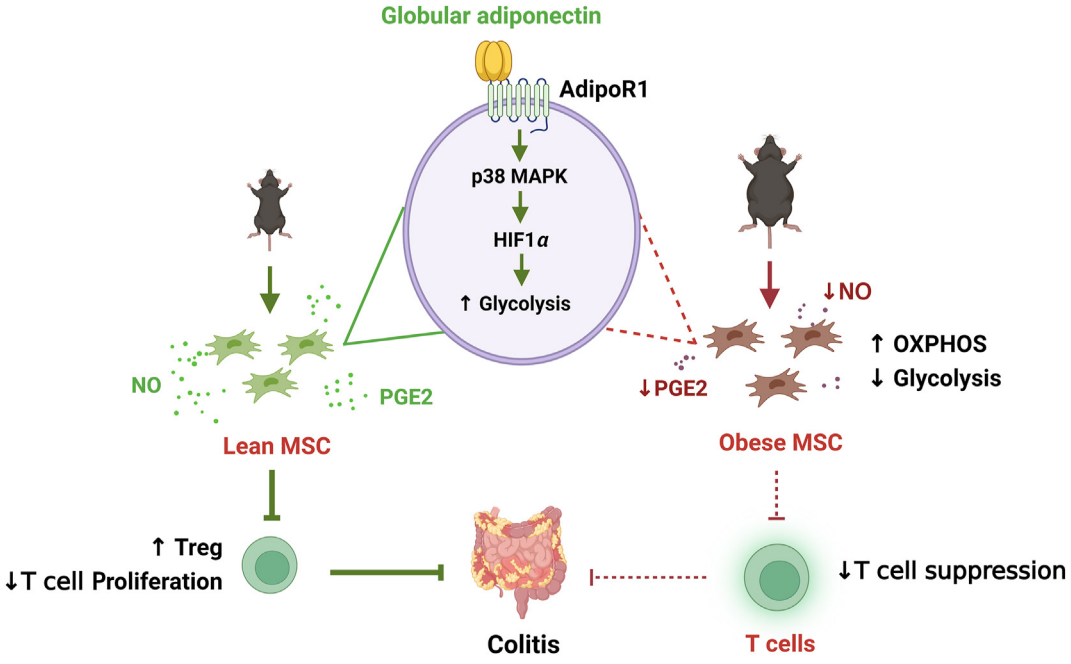

Figure 8 Proposed model for the modulation of immunomodulatory and therapeutic potentials of ADSC by adiponectin under physiological and obese conditions. ADSC isolated from lean mice exert potent immunosuppressive function by regulating T cell proliferation, but inducing differentiation of Treg. In contrast, ADSC derived from obese mice exhibit a compromised immunomodulatory potency, partly due to altered metabolic profile, such as enhanced OXOPHOS, but suppressed glycolysis, which are promoted by obese environment. Pretreatment with adiponectin stimulates the immunomodulatory properties of lean ADSC *via* glycolytic metabolic reprogramming and enhances the therapeutic efficacy against colitis. Interestingly, adiponectin also results in recovery of dysregulated function of ADSC derived from the obese mice. Mechanistically, adiponectin activates AdipoR1/p38MAPK/HIF1α signaling pathway and thereby boosts glycolytic capacity in lean ADSC and recovers metabolic profile of obese ADSC. Given that serum adiponectin is significantly lowered in obese individuals, these findings suggest that dysfunction of obese ADSC may be ascribed to impaired adiponectin signaling by excess adiposity and re-activation of adiponectin signaling would be a promising strategy to enhance therapeutic potentials of these multipotent cells.

whether normalization of serum adiponectin levels in obese individuals can reverse obesity-induced functional abnormalities of MSC. Likewise, while we found that preconditioning with gAcrp restored the therapeutic potential of obese ADSC, this finding has not been validated in mice with obesity. Since obesity was considered a possible risk factor of colitis[49,50], it would be interesting to investigate whether these modified stromal cells are increasingly effective against obesity-associated colitis. Furthermore, this future approach would help draw a clearer conclusion on the possibility of using the modified ADSC for autologous transplantation in obese patients[51]. Another limitation of this study is that the conclusions derived from lean and obese mice need to be confirmed using human MSC. Although animal models help eliminate heterogeneity in the genetic and disease backgrounds of donors, there exist differences in immunomodulatory properties between human and rodent MSC. For example, suppression of lymphocyte proliferation by human MSC is mainly mediated *via* IDO, whereas modulation by rodent MSC is believed to be due to NO secretion[52,53].

5. Conclusions

In summary, the present study sheds light on the modulation of the immunosuppressive function of MSC by adiponectin. On the one hand, adiponectin enhances immunomodulatory potential of normal ADSC through upregulation of molecules responsible for the control of cell-to-cell contact and contact-independent inhibition of immune cell activation. In addition, survival of ADSC under inflammatory environment was improved by adiponectin, which provides further therapeutic advantage for MSC therapy in the treatment of inflammation-associated disorders such as colitis. On the other, adiponectin recovered the immunomodulatory potency of ADSC derived from obese mice by reversion of obesity-induced energy metabolic remodeling to maintain glycolytic flux (Fig. 8). Mechanistically, the adiponectin-enhanced cell viability and immunosuppressive effect of ADSC were mediated *via* activation of the AdipoR1/p38MAPK/HIF1α axis. Taken together, these findings highlight the critical role of adiponectin signaling in regulating the immunomodulatory properties of MSC under basal and obese conditions, and further suggest that preconditioning with adiponectin is a promising strategy for enhancing the effectiveness of MSC therapy against inflammatory and autoimmune diseases.

Acknowledgments

This work was supported by the Basic Science Research Program of the National Research Foundation of Korea (NRF) (NRF-2021R1A2C1013132) and Basic Science Research Program through the National Research Foundation of Korea (NRF) (2020R1A6A1A03044512). The authors thank the Core Research Support Center for Natural Products and Medical Materials (CRCNM) for the technical support regarding the confocal microscopic analysis.

Author contributions

Duc-Vinh Pham: designed and conducted the experiments and wrote the manuscript; Thi-Kem Nguyen: conducted the experiments; Bao-Loc Nguyen: conducted the experiments; Jong-Oh Kim: conceived the idea and designed the experiments; Jee-Heon Jeong: conceived the idea and designed the experiments; Inho Choi: conceived the idea and designed the experiments; Pil-Hoon Park: supervised the project, designed the experiments, and wrote the manuscript.

Conflicts of interest

The authors declare no conflicts of interest.

Appendix A. Supporting information

Supporting data to this article can be found online at https://doi.org/10.1016/j.apsb.2023.10.019.

References

1. Uccelli A, Moretta L, Pistoia V. Mesenchymal stem cells in health and disease. *Nat Rev Immunol* 2008;**8**:726−36.
2. Pittenger MF, Discher DE, Péault BM, Phinney DG, Hare JM, Caplan AI. Mesenchymal stem cell perspective: cell biology to clinical progress. *NPJ Regen Med* 2019;**4**:22.
3. Weiss ARR, Dahlke MH. Immunomodulation by mesenchymal stem cells (MSCS): mechanisms of action of living, apoptotic, and dead MSCS. *Front Immunol* 2019;**10**:1191.
4. López-García L, Castro-Manrreza ME. TNF-α and IFN-γ participate in improving the immunoregulatory capacity of mesenchymal stem/-stromal cells: importance of cell-cell contact and extracellular vesicles. *Int J Mol Sci* 2021;**22**:9531.
5. Blüher M. Obesity: global epidemiology and pathogenesis. *Nat Rev Endocrinol* 2019;**15**:288−98.
6. Perez LM, Bernal A, de Lucas B, San Martin N, Mastrangelo A, Garcia A, et al. Altered metabolic and stemness capacity of adipose tissue-derived stem cells from obese mouse and human. *PLoS One* 2015;**10**:e0123397.
7. Alessio N, Acar MB, Demirsoy IH, Squillaro T, Siniscalco D, Bernardo GD, et al. Obesity is associated with senescence of mesenchymal stromal cells derived from bone marrow, subcutaneous and visceral fat of young mice. *Aging (Albany NY)* 2020;**12**:12609−21.
8. Pérez LM, Suárez J, Bernal A, de Lucas B, San Martin N, Gálvez BG. Obesity-driven alterations in adipose-derived stem cells are partially restored by weight loss. *Obesity* 2016;**24**:661−9.
9. Strong AL, Bowles AC, Wise RM, Morand JP, Dutreil MF, Gimble JM, et al. Human adipose stromal/stem cells from obese donors show reduced efficacy in halting disease progression in the experimental autoimmune encephalomyelitis model of multiple sclerosis. *Stem Cell* 2016;**34**:614−26.
10. Zhu XY, Klomjit N, Conley SM, Ostlie MM, Jordan KL, Lerman A, et al. Impaired immunomodulatory capacity in adipose tissue-derived mesenchymal stem/stromal cells isolated from obese patients. *J Cell Mol Med* 2021;**25**:9051−9.
11. Fasshauer M, Blüher M. Adipokines in health and disease. *Trends Pharmacol Sci* 2015;**36**:461−70.
12. Pham DV, Park PH. Recent insights on modulation of inflammasomes by adipokines: a critical event for the pathogenesis of obesity and metabolism-associated diseases. *Arch Pharm Res (Seoul)* 2020;**43**:997−1016.
13. Oh DK, Ciaraldi T, Henry RR. Adiponectin in health and disease. *Diabetes Obes Metabol* 2007;**9**:282−9.
14. Tian XQ, Yang YJ, Li Q, Huang PS, Li XD, Jin C, et al. Globular adiponectin inhibits the apoptosis of mesenchymal stem cells induced by hypoxia and serum deprivation *via* the adipor1-mediated pathway. *Cell Physiol Biochem* 2016;**38**:909−25.
15. Zhao L, Fan C, Zhang Y, Yang Y, Wang D, Deng C, et al. Adiponectin enhances bone marrow mesenchymal stem cell resistance to flow shear stress through amp-activated protein kinase signaling. *Sci Rep* 2016;**6**:28752.
16. Nakamura Y, Kita S, Tanaka Y, Fukuda S, Obata Y, Okita T, et al. Adiponectin stimulates exosome release to enhance mesenchymal stem-cell-driven therapy of heart failure in mice. *Mol Ther* 2020;**28**:2203−19.
17. Chen T, Wu YW, Lu H, Guo Y, Tang ZH. Adiponectin enhances osteogenic differentiation in human adipose-derived stem cells by activating the APPL1−AMPK signaling pathway. *Biochem Biophys Res Commun* 2015;**461**:237−42.
18. Lee HW, Kim SY, Kim AY, Lee EJ, Choi JY, Kim JB. Adiponectin stimulates osteoblast differentiation through induction of COX2 in mesenchymal progenitor cells. *Stem Cell* 2009;**27**:2254−62.
19. Pham DV, Park PH. Adiponectin triggers breast cancer cell death *via* fatty acid metabolic reprogramming. *J Exp Clin Cancer Res* 2022;**41**:9.
20. Tran VTH, Pham DV, Choi DY, Park PH. Mitophagy induction and aryl hydrocarbon receptor-mediated redox signaling contribute to the suppression of breast cancer cell growth by taloxifene *via* regulation of inflammasomes activation. *Antioxidants Redox Signal* 2022;**37**:1030−50.
21. Lee S, Pham DV, Park PH. Sestrin2 induction contributes to anti-inflammatory responses and cell survival by globular adiponectin in macrophages. *Arch Pharm Res (Seoul)* 2022;**45**:38−50.
22. Hidalgo-Cantabrana C, Algieri F, Rodriguez-Nogales A, Vezza T, Martínez-Camblor P, Margolles A, et al. Effect of a ropy exopolysaccharide-producing *Bifidobacterium animalis* subsp. *lactis* strain orally administered on DSS-induced colitis mice model. *Front Microbiol* 2016;**7**:868.
23. Kim JJ, Shajib MS, Manocha MM, Khan WI. Investigating intestinal inflammation in DSS-induced model of IBD. *J Vis Exp* 2012;**1**:3678.
24. Pham DV, Shrestha P, Nguyen TK, Park J, Pandit M, Chang JH, et al. Modulation of NLRP3 inflammasomes activation contributes to improved survival and function of mesenchymal stromal cell spheroids. *Mol Ther* 2023;**31**:890−908.
25. Engeli S, Feldpausch M, Gorzelniak K, Hartwig F, Heintze U, Janke Jr , et al. Association between adiponectin and mediators of inflammation in obese women. *Diabetes* 2003;**52**:942−7.
26. Song N, Scholtemeijer M, Shah K. Mesenchymal stem cell immunomodulation: mechanisms and therapeutic potential. *Trends Pharmacol Sci* 2020;**41**:653−64.
27. Lv B, Li F, Fang J, Xu L, Sun C, Han J, et al. Hypoxia inducible factor 1α promotes survival of mesenchymal stem cells under hypoxia. *Am J Transl Res* 2017;**9**:1521−9.
28. Taylor CT, Scholz CC. The effect of HIF on metabolism and immunity. *Nat Rev Nephrol* 2022;**18**:573−87.
29. Zhou T, Yuan Z, Weng J, Pei D, Du X, He C, et al. Challenges and advances in clinical applications of mesenchymal stromal cells. *J Hematol Oncol* 2021;**14**:24.
30. Ryu JS, Jeong EJ, Kim JY, Park SJ, Ju WS, Kim CH, et al. Application of mesenchymal stem cells in inflammatory and fibrotic diseases. *Int J Mol Sci* 2020;**21**:8366.
31. Lee BC, Kang KS. Functional enhancement strategies for immunomodulation of mesenchymal stem cells and their therapeutic application. *Stem Cell Res Ther* 2020;**11**:397.
32. Srinivasan A, Sathiyanathan P, Yin L, Liu TM, Lam A, Ravikumar M, et al. Strategies to enhance immunomodulatory properties and reduce heterogeneity in mesenchymal stromal cells during *ex vivo* expansion. *Cytotherapy* 2022;**24**:456−72.
33. Kastrinaki MC, Sidiropoulos P, Roche S, Ringe J, Lehmann S, Kritikos H, et al. Functional, molecular and proteomic characterisation of bone marrow mesenchymal stem cells in rheumatoid arthritis. *Ann Rheum Dis* 2008;**67**:741−9.
34. Murphy JM, Dixon K, Beck S, Fabian D, Feldman A, Barry F. Reduced chondrogenic and adipogenic activity of mesenchymal stem

cells from patients with advanced osteoarthritis. *Arthritis Rheum* 2002;**46**:704−13.
35. Schu S, Nosov M, O'Flynn L, Shaw G, Treacy O, Barry F, et al. Immunogenicity of allogeneic mesenchymal stem cells. *J Cell Mol Med* 2012;**16**:2094−103.
36. Nauta AJ, Westerhuis G, Kruisselbrink AB, Lurvink EG, Willemze R, Fibbe WE. Donor-derived mesenchymal stem cells are immunogenic in an allogeneic host and stimulate donor graft rejection in a non-myeloablative setting. *Blood* 2006;**108**:2114−20.
37. González MA, Gonzalez-Rey E, Rico L, Büscher D, Delgado M. Adipose-derived mesenchymal stem cells alleviate experimental colitis by inhibiting inflammatory and autoimmune responses. *Gastroenterology* 2009;**136**:978−89.
38. Sala E, Genua M, Petti L, Anselmo A, Arena V, Cibella J, et al. Mesenchymal stem cells reduce colitis in mice *via* release of TSG6, independently of their localization to the intestine. *Gastroenterology* 2015;**149**:163−76.e20.
39. Liu J, Lai X, Bao Y, Xie W, Li Z, Chen J, et al. Intraperitoneally delivered mesenchymal stem cells alleviate experimental colitis through THBS1-mediated induction of IL-10-competent regulatory B cells. *Front Immunol* 2022;**13**:853894.
40. Holzwarth C, Vaegler M, Gieseke F, Pfister SM, Handgretinger R, Kerst G, et al. Low physiologic oxygen tensions reduce proliferation and differentiation of human multipotent mesenchymal stromal cells. *BMC Cell Biol* 2010;**11**:11.
41. Lee JH, Yoon YM, Lee SH. Hypoxic preconditioning promotes the bioactivities of mesenchymal stem cells *via* the HIF-1α−GRP78−AKT axis. *Int J Mol Sci* 2017;**18**:1320.
42. Contreras-Lopez R, Elizondo-Vega R, Paredes MJ, Luque-Campos N, Torres MJ, Tejedor G, et al. HIF1α-dependent metabolic reprogramming governs mesenchymal stem/stromal cell immunoregulatory functions. *FASEB J* 2020;**34**:8250−64.
43. Contreras-Lopez R, Elizondo-Vega R, Luque-Campos N, Torres MJ, Pradenas C, Tejedor G, et al. The ATP synthase inhibition induces an ampk-dependent glycolytic switch of mesenchymal stem cells that enhances their immunotherapeutic potential. *Theranostics* 2021;**11**:445−60.
44. Fillmore N, Huqi A, Jaswal JS, Mori J, Paulin R, Haromy A, et al. Effect of fatty acids on human bone marrow mesenchymal stem cell energy metabolism and survival. *PLoS One* 2015;**10**:e0120257.
45. Yamauchi T, Iwabu M, Okada-Iwabu M, Kadowaki T. Adiponectin receptors: a review of their structure, function and how they work. *Best Pract Res Clin Endocrinol Metabol* 2014;**28**:15−23.
46. Hug C, Wang J, Ahmad NS, Bogan JS, Tsao TS, Lodish HF. T-Cadherin is a receptor for hexameric and high-molecular-weight forms of Acrp30/adiponectin. *Proc Natl Acad Sci U S A* 2004;**101**:10308−13.
47. Yamauchi T, Kamon J, Ito Y, Tsuchida A, Yokomizo T, Kita S, et al. Cloning of adiponectin receptors that mediate antidiabetic metabolic effects. *Nature* 2003;**423**:762−9.
48. Lin YY, Chen CY, Chuang TY, Lin Y, Liu HY, Mersmann HJ, et al. Adiponectin receptor 1 regulates bone formation and osteoblast differentiation by GSK-3β/β-catenin signaling in mice. *Bone* 2014;**64**:147−54.
49. Singh S, Dulai PS, Zarrinpar A, Ramamoorthy S, Sandborn WJ. Obesity in IBD: epidemiology, pathogenesis, disease course and treatment outcomes. *Nat Rev Gastroenterol Hepatol* 2017;**14**:110−21.
50. Kim JH, Oh CM, Yoo JH. Obesity and novel management of inflammatory bowel disease. *World J Gastroenterol* 2023;**29**:1779−94.
51. Pham DV, Nguyen TK, Park PH. Adipokines at the crossroads of obesity and mesenchymal stem cell therapy. *Exp Mol Med* 2023;**55**:313−24.
52. Ren G, Su J, Zhang L, Zhao X, Ling W, L'huillie A, et al. Species variation in the mechanisms of mesenchymal stem cell-mediated immunosuppression. *Stem Cell* 2009;**27**:1954−62.
53. Ren G, Zhang L, Zhao X, Xu G, Zhang Y, Roberts AI, et al. Mesenchymal stem cell-mediated immunosuppression occurs *via* concerted action of chemokines and nitric oxide. *Cell Stem Cell* 2008;**2**:141−50.